EFFECTS OF *pennisetum purpureum* LEAF EXTRACT ON CYTOKINE AND IMMUNE CELL RESPONSES IN CYCLOPHOSPHAMIDE-INDUCED IMMUNOSUPPRESSION IN RATS

BY

EZEOHA, CHIDUBEM, ERNEST
GOU/U22/BCH/23

DEPARTMENT OF CHEMICAL SCIENCES, FACULTY OF NATURAL SCIENCE AND ENVIRONMENTAL STUDIES
GODFREY OKOYE UNIVERSITY
UGWUOMU-NIKE, ENUGU

A PROJECT RESEARCH SUBMITTED TO THE DEPARTMENT OF CHEMICAL SCIENCES IN PARTIAL FULFILMENT OF THE REQUIREMENTS FOR THE AWARD OF BACHELOR OF SCIENCE (B.Sc.) DEGREE IN INDUSTRIAL CHEMISTRY

SUPERVISOR: DR. ELEAZAR . C. ANORUE

JULY, 2026

APPROVAL PAGE

This project effects of *pennisetum purpureum* leaf extract on cytokine and immune cell responses in cyclophosphamide-induced immunosuppression in rats has been approved for the award of the degree of Bachelor of Science in Biochemistry, Godfrey Okoye University Enugu, Nigeria.

BY

Dr. Eleazar . C. Anorue	…….	……
Project Supervisor	Signature	Date

Dr. Joy Anosike	…….	……
Head of Department	Signature	Date

Prof. Chidi Uhuegbu	…….	……
Dean Faculty of NSES	Signature	Date

	…….	……
EXTERNAL EXAMINER	Signature	Date

CERTIFICATION

I certify that this project work was carried out by Ezeoha Chidubem Ernest with Registration number GOU/U22/BCH/23 in the department of chemical sciences, Faculty of Natural Science and Environmental Studies, Godfrey Okoye University, Enugu, in fulfillment of the requirement for the award of Bachelors Degree in Science (B. Sc.).

Dr. Eleazar . C. Anorue	…….	……
Project Supervisor	Signature	Date

Dr. Joy Anosike	…….	……
Head of Department	Signature	Date

Prof. Chidi Uhuegbu	…….	……
Dean Faculty of NSES	Signature	Date

	…….	……
EXTERNAL EXAMINER	Signature	Date

DEDICATION

This work is dedicated to my family who has been of great support to this project work, with the help of the almighty and intercession of our Blessed Mother Mary.

ACKNOLEDGEMENT

In sincere gratitude, I thank God almighty for his ever present help and for the special gift of the holy spirit, and our Mother Mary for her intercession throughout my academic pursuit and in the process of this project work.

My unalloyed gratitude goes to my supervisor Dr .Eleazar Anorue and H.O.D Dr. Joy Anosike for their constant encouragement, advice, availability, consistency and patience for believing in my potentials.

My appreciation also goes to my lecturers, Dr. Chidinma, Dr. Agbara , who has been a source of inspiration for me to strive for the best. I also want to thank all my teachers in chemistry laboratory the for their support and advice especially, Aunty Amara , Mr Jachi .

ABSTRACT

The present study evaluated the immunomodulatory effects of the ethanolic leaf extract of *Pennisetum purpureum* in cyclophosphamide-induced immunosuppression Wistar albino rats. Thirty-five male rats were assigned into seven groups and treated with 100, 200, or 400 mg/kg of the extract, Levamisole, or appropriate controls for 14 days. Immunological parameters including serum interleukin-6 (IL-6), immunoglobulin M (IgM), and $CD4^+$ T-cell counts were assessed. Phytochemical constituents were identified by GC-MS, while molecular docking and SwissADME analyses were performed to evaluate the binding affinity and pharmacokinetic properties of the identified compounds.Cyclophosphamide significantly increased IL-6 while reducing IgM and $CD4^+$ T-cell counts ($p < 0.05$). Treatment with *Pennisetum purpureum* extract significantly and dose-dependently reduced IL-6 and restored IgM and $CD4^+$ T-cell levels, with the 400 mg/kg dose producing effects comparable to the normal control and the reference drug, Levamisole. GC-MS identified fifteen bioactive compounds, of which eight demonstrated stronger binding affinities to the IgM target than Levamisole. Most compounds also exhibited favourable drug-likeness and pharmacokinetic profiles.The findings demonstrate that the ethanolic leaf extract of *Pennisetum purpureum* possesses significant dose-dependent immunomodulatory activity, with phytosterols likely contributing to its therapeutic effects. These results support the plant's potential as a source of novel immunomodulatory agents and warrant further isolation, mechanistic, and toxicological studies.

Keywords: Pennisetum purpureum, Immunomodulation, Cyclophosphamide, Interleukin-6, Immunoglobulin M, $CD4^+$ T-cells, GC-MS, Molecular Docking, Phytosterols.

TABLE OF CONTENTS

CHAPTER THREE: MATERIALS AND METHODS

CHAPTER FOUR: RESULTS

CHAPTER FIVE: DISCUSSION AND CONCLUSION

LIST OF TABLES

LIST OF FIGURES

Figure 31: 2D diagram showing only one Pi-alkyl interactions for Levamisole and IgM protein residue at the active sites (ALA 539 and five (5) weak Van der Waal interactions at PHE 485, GLU 541, ASP 483, VAL 484 and HIS 540). Similarly, there are no hydrogen bond interactions between Levamisole and the residue and fewer interactions compared with Levamisole resulted in very low binding energy of -4.8 kcal/mol as shown in the docking results. However, generally there were six (6) sites of interactions.

Figure 32: 3D diagram showing the structure of Levamisole docked with IgM protein residue. As can be observed from the diagram, the compound did not fit in too well in the residue which resulted in a very low binding affinity.

CHAPTER ONE

INTRODUCTION

1.1 Background of the Study

The immune system is a complex and extremely controlled network of cells, tissues and biochemical mediators that contribute to homeostasis and defense of the body against pathogens and foreign materials. It is composed of innate and adaptive elements which work in a concerted way to identify and get rid of destructive agents. Cytokines like interleukin-6 (IL-6), are central to the regulation of immune functions, as they play significant roles in mediating inflammatory response, activating immune cells, as well as orchestrating host defenses (Kumar *et al* ., 2022). Moreover, Immunoglobulins, especially Immunoglobulin M (IgM), are the key indicators of humoral immunity and the signs of the ability to produce antigen-specific immune responses (Sharma and Sharma, 2023).

Although efficient, the immune system can be impaired by a number of variables including diseased state, environmental stressors, and pharmacological agents. Cyclophosphamide is one of the most commonly used immunosuppressive agents in clinical and in experimental practice. Cyclophosphamide is an alkylating agent that has cytotoxic effects, as it interferes with the replication of DNA, thus inhibiting speedily dividing cells, like the immune cells. Even though it has a therapeutic application in the treatment of cancers and autoimmune diseases, its use is linked to severe immunosuppression, which is manifested by a decline in the production of cytokines, a depreciate in the number of white blood cells, as well as the production of antibodies (Singh and Singh, 2021). Consequently, a widely accepted experimental model in assessing the effectiveness of immunomodulatory agents has been the cyclophosphamide-induced immunosuppression.

Over the past few years, the utilization of medicinal plants as a substitute or complementary in the regulation of immune responses has gained interest. Plant-derived compounds have been discoverd to have great immunomodulatory, antioxidant, and anti-inflammatory effects including flavonoids, alkaloids, saponins, and phenolic compounds (Batiha *et al* ., 2020; Anand *et al* ., 2023). The mechanisms of these bioactive constituents are that they have the ability to stimulate immune signaling pathways such as nuclear factor kappa B (NF-KB) and regulate the production of cytokines, thereby improving the activity of immune cells (Khan *et al* ., 2021; Rashid and Cho, 2021). Experimental evidence also indicates that these compounds have the potential to revitalize immune response in immunosuppressed states by enhancing the production of cytokines, antibodies, and lymphocyte growth (Choudhary *et al* ., 2022).

Pennisetum purpureum is a perennial tropical grass that is commonly referred to as elephant grass, is a relative of the family *Poaceae* and is extensively spread in areas like Nigeria. Even though it is mainly known as an agricultural commodity since it serves as livestock feed, recent research has revealed that it has a range of phytochemicals (flavonoids, tannins, saponins, phenolic compounds) that are linked to several biological activities (Nwodo *et al* ., 2021). These components have been reported to have antioxidant and anti-inflammatory effects, implying that they may have immunomodulatory effects.

The development of analytical and computation methods has greatly contributed to the analysis of medicinal plants and their pharmacological values. By using analytical tools such as Gas Chromatography-Mass Spectrometry (GC-MS), phytochemical components of plant extracts can be identified and characterized, establishing a link between the chemical makeup and the biological effects of the plant extracts (Patel and Patel, 2022). Moreover, Molecular Docking has become an effective in silico method to anticipate the interaction among bioactive compounds

and biological targets, such as cytokine receptors and inflammatory mediators. This methodology offers mechanistic evidence of the immunomodulatory capabilities of plant-derived substances and helps back up experimental results (Li et al ., 2023; Yadav et al ., 2024).
The recent findings validate the importance of using in vivo, analytical and computational research methods to evaluate in a comprehensive manner therapeutic potential of medicinal plants (Anand et al ., 2023). In spite of these developments, there is still a dearth of data specifically focused on immunomodulatory actions of *Pennisetum purpureum* leaves especially in cytokine modulation, humoral immunity, and molecular interactions with immune targets.

Therefore, the study evaluates the immunomodulatory activity of *Pennisetum purpureum* leaves on cyclophosphamide-induced immunosuppressed rats by estimation of the key immune parameters such as IL-6, IgM and immune cell markers and identification of bioactive compounds from *Pennisetum purpureum* leaves by GC-MS and their interaction with immune cell targets by molecular docking.

1.2 Statement of the Problem

The immunosuppression is linked with the predisposition to infections, slowed recovery, and deteriorated physiological performance. Even though there are traditional immunomodulatory drugs, their application is frequently restricted due to side effects, high price, and decreased accessibility. Although cyclophosphamide is a good chemotherapeutic agent, it causes serious impairment of immune function, which results in low levels of cytokines, low levels of immunoglobulins, and low activity of immune cells (Singh and Singh, 2021).

Medicinal plants have also demonstrated potential as safer substitutes, but the immunomodulatory effects of medicinal plants (especially of *Pennisetum purpureum*) have little

scientific validation. In addition, there are limited papers that have used an integrated methodology that involves biochemical tests, phytochemical tests, and computational studies. This disparity highlights the importance of the extensive research to assess the immunomodulatory effect of this plant.

1.3 Aim of the Study

To evaluate the immunomodulatory effects of *Pennisetum purpureum* leaves in cyclophosphamide-induced immunosuppression in rats.

1.4 Objectives of the Study

The specific objectives are to:

I. To determine the effect of the extract on cytokine levels of the immunosuppressed rats.
II. To determine the effects of the extract on immune cell markers of the immunosuppressed rats.
III. To characterize the bioactive principles in the extract using Gas Chromatogragpy-Mass Spectometry
IV. To determine the binding affinity of the identified bioactive principles to the immune related target protein

1.5 Research Hypothesis

I. Null Hypothesis (H 0): *Pennisetum purpureum* leaves do not cause any significant immunomodulatory effect in the cyclophosphamide-induced immunosuppression rats.
II. Alternative Hypothesis (H): *Pennisetum purpureum* leaves have profound immunomodulatory effects on the immunosuppressed rats induced by cyclophosphamide.

1.6 Significance of the Study

This study may generate valuable scientific evidence regarding the immunomodulatory effects of *Pennisetum purpureum*. By integrating immunological, phytochemical and molecular docking analyses' the findings could provide a basis for further studies on it's bioactive principles, mechanisms of action and potential therapeutic applications.

1.7 Scope of the Study

To achieve the aim of this study, the research evaluated selected cytokines and immune cell markers in cyclophosphamide-induced immunosuppression in rats treated with *Pennisetum purpureum* leaf extract. The study also characterized the phytochemical constituents of the extract using GC-MS analysis and investigate the interactions of identified bioactive principles with immune-related target proteins through molecular docking analysis.

1.8 Justification of the Study

Conventional immunomodulatory drugs are associated with limitations such as bone marrow suppression, hepatotoxicity and gastrointestinal distress , hence the need for exploration of safer alternative therapeutic agents .given the ethnomedicinal use and phytochemical richness of *Pennisetum purpureum* in immune modulation and provide a foundational framework for further studies and validation of the plant extract as a potential immunomodulatory agent.

CHAPTER TWO

LITERATURE REVIEW

2.1 Conceptual Review

2.1.1 Detailed Overview of the Immune System

The immune system is a complex and dynamic biological web comprising cells, tissues, organs, and chemical signals that act in concert to defend the body against pathogens, toxins, and abnormal cells while preserving physiological homeostasis. Immune competence depends on a balance between activation and regulation, self-tolerance, and coordinated communication between cellular and molecular components (Kumar *et al* ., 2022).

Structural Organisation of the Immune System

Lymphoid organs are classifed as primary (central) and secondary (peripheral) organs. Immune cell production and maturation occurs in primary lymphoid organs like the thymus and bone marrow. Immune activation and antigen recognition materialize in secondary lymphoid organs, comprising the spleen, lymph nodes, and mucosa-associated lymphoid tissues. Since the spleen is a significant source of IgM production during primary immunological responses and the effects of cyclophosphamide on the spleen have frequently been utilized as a marker of immunosuppression, the spleen is a location of particular relevance in our investigation (Emadi et al., 2009).

Innate Immunity: First Line of Defence

The innate immune system has a quick reaction to the intuding pathogens, using pattern recognition receptors (PRRs) that recognize pathogen associated molecular patterns (PAMPs) in a non-specific manner. Important cell components include dendritic cells, neutrophils, macrophages, and natural killer cells (NK cells). The innate response is amplified by soluble mediators such the complement proteins and cytokines. Phagocytes comprise macrophages and neutrophils, which play a essential role in the phagocytosis of microorganisms, and dendritic cells, which link innate and adaptive immune systems by bringing up antigens to T cells (Kumar et al., 2022).

Interleukin-6 as a Central Regulatory Cytokine

The pleiotropic cytokine IL-6 is particularly important in the control of innate immunity. IL-6 is generated by macrophages, T cells, and endothelial cells in response to tissue injury, immunological activation, or infection. In the setting of classical IL-6 receptor signaling (membrane-bound IL-6R), cytokines with mostly pro-inflammatory effects also have anti-inflammatory and reparative capabilities; however, soluble IL-6R is an axis that is primarily pro-inflammatory (Rose-John, 2021; Hunter and Jones, 2015).

An important aspect of this study was that IL-6 is a principal regulator of B-cell differentiation to antibody producing plasma cells, therefore precisely linked to Immunoglobulin M (IgM) generation during primary immune responses. The action of cyclophosphamide is also upstream of the IgM decline seen in immunosuppressed animals, by suppressing the production of IL-6, which is due to the killing of rapidly dividing lymphocytes. Therefore, the restoration of IL-6 levels can be used directly as a marker of cytokine recovery, and indirectly as a marker of IgM recovery, (Rose-John, 2021). This is why IL-6 is the main cytokine investigated in this work, and

because it is coupled with the measurement of IgM it offers a logically coherent measure of humoral immune recovery.

Adaptive Immunity: Specific and Memory-Based Response

B and T cells mediate antigen-specific responses provided by the adaptive immune system. T helper cells (CD4+) control this process by secreting cytokines, while cytotoxic T cells (CD8+) eradicate aberrant or septic cells. B cells evolve into plasma cells and discahrge antibodies. Because B-cell antibody production (IgM) and T-cell cytokine output (especially IL-6 from helper T cells) are interdependent, assessing both parameters at the same time offers a thorough and mechanistically coherent picture of adaptive immune activity (Kumar et al., 2022).

Immune System in Health and Disease

Dysregulation of the immune system produces a spectrum of conditions ranging from chronic inflammation and autoimmune disease to immunodeficiency and infection susceptibility. Drug-induced immunosuppression, such as that produced by cyclophosphamide, replicates several features of acquired immunodeficiency and provides a reproducible experimental framework for evaluating immunomodulatory interventions (Singh and Singh, 2021).

2.1.2 Cellular Components of Immunity

The immune system is composed of diverse specialised cells that collectively mediate pathogen recognition, immune activation, and resolution. These cellular components are broadly categorised into innate and adaptive immune cells, each contributing distinct but interconnected functions.

Phagocytic Cells

The most prevalent leukocytes in circulation are neutrophils, which easily move to infection sites in response to chemotactic cues. Through phagocytosis, degranulation, and the propagation of reactive oxygen species to eradicate pathogens, they contribute significantly to acute inflammation. The tissue-resident cells known as macrophages, which perform phagocytosis, secrete cytokines like IL-6, and present antigens, are produced by monocytes and act as a link between innate and adaptive immunity. Cyclophosphamide models are characterized by neutrophilia and monocytosis (Kumar et al., 2022).

Lymphocytes: The Adaptive Immune Effectors

B lymphocytes mediate humoral immunity by producing plasma cells, which then make immunoglobulins. Since IgM is the first type of antibody produced when the body first encounters a novel antigen and is the first to be reduced by cyclophosphamide-induced B-cell depletion, it is the most sensitive early indicator of humoral immune activity (Sharma and Sharma, 2023). T helper cells (CD4+) use cytokines, particularly IL-6, which is crucial for plasma cell development, to signal B-cell activation and antibody class switching. Cytotoxic T cells (CD8+) use cytotoxic chemicals to destroy tumor or contaminated cells. The natural killer (NK) cells are not sensitised and provide surveillance activity against virus infected and transformed cells (Kumar et al ., 2022).

Granulocytes and Monocytes

While basophils release inflammatory mediators (like histamine), eosinophils take role in allergic reactions and anti-parasitic immunity. Monocytes play a essential function in immunological observation, antigen presentation, and cytokine synthesis. They also serve as circulating progenitors to macrophages and dendritic cells. Total and differential white blood cell (WBC) counts, which include neutrophils, lymphocytes, and monocytes, are crucial haematological

indices used in experiments to assess the animals' immune systems (Singh and Singh, 2021; Choudhary et al., 2022).

Immune Cell Markers in Experimental Studies

In the context of cyclophosphamide-induced immunosuppression leukopenia and lymphocytopenia are characteristic features, in that they indicate impaired haematopoiesis and destruction of lymphocytes. Recovery of these cells after treatment with an immunomodulatory agent represents an increase in immune competence and haematopoietic recovery. Together with cytokine quantification (IL-6) and antibody measurement (IgM), immune cell counts provide an integrated, multi-level assessment of immunomodulatory activity (Anand et al ., 2023).

2.1.3 Immunosuppression and Experimental Models

Immunosuppression is a condition of suppressed or weakened immune system and a decreased ability to produce normal immune responses to pathogens, toxins, or abnormal cells. Experimental immunosuppression is surgical deprivation to test the effectiveness of immunomodulatory agents in a reproducible controlled environment (Singh and Singh, 2021).

Classification of Immunosuppression

There are two types of immunosuppression: primary (congenital), which results from an immune system malfunction, and secondary (acquired), which is brought on by external factors such infections, drug usage, environmental stress, or starvation. The drug-induced immunosuppression paradigm is the most widely used animal model in experimental pharmacology due to its great reproducibility and clearly defined mechanistic objectives (Choudhary et al., 2022).

Cyclophosphamide-Induced Immunosuppression: Mechanisms and Rationale for IgM as the Primary Antibody Endpoint

Cyclophosphamide is an alkylating agent which interferes with DNA strand cross linking and selectively kills rapidly proliferating cells. Among the immune system, this mainly affects bone marrow progenitors and activated lymphocytes, which causes: leukopenia and lymphocytopenia; an inhibitory effect on the secretion of IL-6 by macrophages; reduction of the number of lymphocytes in bone marrow and the spleen; and atrophy of the spleen and thymus (Emadi et al ., 2009; Baharara et al ., 2017).

This is because in the case of cyclophosphamide the use of IgM as the main antibody endpoint is directly related to the biology of cyclophosphamide-induced immunosuppression. IgM is the first antibody isotype secreted by newly-activated B lymphocytes in primary immune responses, before the generation of immunological memory or class switching to IgG. Important, cyclophosphamide selectively targets early B cells, the cells that make IgM, but leaves memory B cells and more differentiated plasma cells that make IgG relatively unaffected. Thus, IgM levels are the most biologically relevant and mechanistically most sensitive antibody marker of this model, because it is the antibody produced by the most profoundly depleted compartment, which is the naive B-cell compartment. In such cases, the level of IgG would rather indicate underlying residual memory responses that can last even after continuing to take immunosuppression; what this implies is that the level of immune compromise will be underestimated (Sharma and Sharma, 2023; Emadi et al ., 2009).

In addition, cyclophosphamide inhibits the production of IL-6, which is the most important cytokine for B-cell differentiation into IgM-producing plasma cells during primary responses, thus acting mechanistically upstream of the suppression of IgM production. This

establishes a biological pathway, cyclophosphamide → suppression of IL-6 → depletion of IgM → impaired early humoral immunity, which may be argued as the basis for proceeding with combined measurement of both IL-6 and IgM as paired endpoints in this study.

Measurable Parameters and Study Design

The present study evaluates immune function using: serum IL-6 as the primary cytokine indicator of innate-to-adaptive immune signalling; serum IgM as the primary humoral immunity marker reflecting early B-cell function; total WBC and differential counts as haematological indices of haematopoietic recovery; and histological examination of the spleen and thymus as structural indicators of lymphoid organ integrity. Improvement across all four parameter groups following treatment with *Pennisetum purpureum* leaf extract will constitute evidence of immunostimulatory activity (Choudhary *et al* ., 2022).

Alternative Models of Immunosuppression

Other experimental immunosuppression models include glucocorticoid-induced models (dexamethasone), radiation-induced lymphodepletion, stress-induced hormonal immunosuppression, and pathogen-induced models. Each offers unique mechanistic insights, but cyclophosphamide remains preferred because its mechanism is well-characterised, the resulting immune deficits are reproducible and quantifiable, and it mimics the immunosuppression experienced by cancer patients receiving chemotherapy — a clinically relevant context for testing natural immunomodulatory agents (Anand *et al* ., 2023).

2.1.4 Mechanisms of Immunomodulation

Immunomodulation refers to the biological mechanisms that regulate, strengthen or weaken the immune system so that it responds appropriately and balanced. In this study, the emphasis is on

immunostimulation, in particular on the restoration of suppressed immune function in cyclophosphamide treated animals. There are several molecular, cellular and systemic mechanisms of immunomodulatory activity, which may have a more synergistic effect (Anand et al., 2023).

IL-6 Pathway Modulation and B-Cell Activation

In this model, the IL-6 signalling pathway acts as a link between innate cytokine production and adaptive humoral immunity. Macrophage derived IL-6 is greatly diminished after cyclophosphamide in immunosuppressed states, leading to poor B-cell differentiation, and hence low IgM-secretion. The immunomodulatory phytochemicals like flavonoids can stimulate macrophages by modulating the NF-κB pathway to restore IL-6 production and thus to re-activate the IL-6–IgM signalling axis (Rose-John, 2021; Kumar et al ., 2022). Quercetin, luteolin and apigenin, specific subclasses of flavonoids, have been identified as being able to induce the upregulation of IL-6 in quiescent macrophage culture at physiologically relevant concentrations (Panche et al ., 2016).

Stimulation of Immune Cell Proliferation

Plant derived immunomodulatory agents can promote haematopoietic recovery by stimulating proliferation of bone marrow progenitors and peripheral lymphocytes. This causes a rise in both the number of lymphocytes and total WBCs which is due more to restoration of immune cell

production than any redistribution. Saponins are known to improve the activity of macrophages and proliferation of lymphocytes via the activation of toll-like receptors, apart from their antioxidant activity (Anand et al ., 2023).

Antioxidant Mechanisms Supporting Immune Recovery

A side effect of the metabolism of cyclophosphamide is the generation of reactive oxygen species (ROS). This damaging effect is compounded by the direct cytotoxic effect, as oxidative by-products occur and damage the haematopoietic progenitors, lymphocytes, and lymphoid organs. Plants extracts with their phenolic compounds and flavonoids remove these free radicals by donating electrons and chelating metal ions, thus preventing the immune cells from being destroyed by these free radicals and helping to promote healing. The antioxidant mechanism works outside the direct immunostimulatory mechanisms on cytokine production (Ajiboye et al ., 2021).

Modulation of NF-κB and Intracellular Signalling Pathways

Multiple intracellular signalling pathways govern the expression of immune-relevant genes and cytokines. The NF-κB pathway regulates transcription of IL-6 and other pro-inflammatory mediators and is a primary target for plant-derived immunomodulatory compounds. MAPK pathways influence cell proliferation, differentiation, and inflammatory gene expression. Flavonoids and phenolic acids modulate both pathways, with the net effect in immunosuppressed

states being the restoration of baseline cytokine signalling rather than pro-inflammatory overstimulation (Kumar *et al* ., 2022; Anand *et al* ., 2023).

2.2 *Pennisetum purpureum* Schumach.: Botany, Phytochemistry, and Pharmacology

2.2.1 Taxonomy and Classification of Pennisetum purpureum

Pennisetum purpureum Schumach., widely recognized as elephant grass or Napier grass, is a tall perennial tropical grass with the following taxonomic classification:

Kingdom: *Plantae*

Superdivision: *Spermatophyta* (seed plants)

Division: *Magnoliophyta* (angiosperms)

Class: *Liliopsida* (monocotyledons)

Order: *Poales*

Family: *Poaceae*

Genus: *Pennisetum*

Species: *Pennisetum purpureum Schumach.*

This classification places the plant within *Poaceae*, a family of considerable economic and pharmacological importance encompassing major food crops and numerous plants with documented bioactive secondary metabolites (Batiha *et al* ., 2020). Some botanical systems have reclassified the species as Cenchrus purpureus; however, *Pennisetum purpureum* remains the accepted name in most agricultural and pharmacological literature, particularly across Africa (Nwodo *et al* ., 2021).

2.2.2 Morphological Description and Ecological Distribution

Pennisetum purpureum is a tufted and highly vigorous species of grass which, under ideal conditions, reaches a height of 3 to 7 metres and is one of the tallest of tropical grasses. It has the following structural features:

Stem (Culms): Erect, thick, fibrous, segmented with prominent nodes where the lateral stems grow from and where vegetative propagation by stem cutting takes place.

Flowers: Large, umbel-like, drooping, and pink, with petals that are pointed and wavy.Leaves are long and narrow, linear-lanceolate, 30-120cm with rough margins, prominent midrib and slightly hairy surface. The characteristics decrease transpiration and increase mechanical toughness of the exposed habitats.

Inflorescence: a terminal cylindrical spikelet that is densely branched and bears a large number of bristle tipped spikelets, making the plant look feathery. Vegetative propagation is the preferred method as seed viability is frequently low.

Root System: Deep and extensive fibrous roots which increase uptake of water and nutrients, soil stability and drought tolerance (Batiha et al., 2020; Nwodo et al., 2021).

From the ecological point of view, *Pennisetum purpureum* requires tropical and subtropical environments, where the temperature is between 25–35°C and rainfall is more than 1000 mm per

year. Very tolerant of loamy, sandy or clay soils and quickly invades grasslands, river banks and disturbed areas. It is especially abundant in West Africa, Nigeria in particular where conditions are favorable for its growth and is extensively grown for fodder and erosion control. These secondary metabolites of pharmacological interest are also part of an increased production of stress-response secondary metabolites related to ecological resilience (Anand et al ., 2023). Under stress conditions, plants have a tendency to produce more of secondary metabolites including flavonoids, phenolics and saponins as a defence mechanism to oxidative stress, UV radiation and herbivores. This ecological-phytochemical relationship forms some of the biological basis for the investigation of immunomodulatory potential of the *Pennisetum purpureum* when grown under the tropical environment of Nigeria (Nwodo et al., 2021).

2.2.3 Phytochemical Constituents of Pennisetum purpureum

Pharmacological relevance of *Pennisetum purpureum* is related to its phytochemistry. The plant contains secondary metabolites like flavonoids, phenolic compounds, saponins, alkaloids, and tannins, which have unique biological activities that are important for immune regulation (Anand et al ., 2023).

Flavonoids

The flavonoids are the most important phytochemical group in *Pennisetum purpureum* from immunologic point of view. Specific subclasses of related Poaceae species with proven ability to regulate IL-6 production and B-cell differentiation include quercetin, luteolin, apigenin and

vitexin. Their immunomodulatory mechanism works mainly by modulating the NF-κB pathway, by inhibiting pro-inflammatory phosphodiesterases and by free radical scavenging activity which prevents the lymphocytes from oxidative damage (Batiha et al., 2020; Panche et al., 2016).

Phenolic Compounds

Hydroxycinnamic acid derivatives and phenolic acids are important phenolic compounds found in the plants that can scavenge reactive oxygen species (ROS) and chelate metals, contributing significantly to the plants' antioxidant activity. Phenolics prevent haematopoietic progenitor cells from ROS induced damage in immune tissues — especially in the context of cyclophosphamide induced ROS damage. Phenolics also regulate the manifestation of inflammatory genes by suppressing the metabolism of arachidonic acid (Nwodo et al., 2021).

Saponins

Saponins are glycosidic molecules reported to have strong adjuvant and immunostimulatory activities. They exert immune effects via activation of the TLRs on macrophages, induction of lymphocyte proliferation and early antibody production (IgM) during primary immune responses. The power to augment primary IgM responses, such as the ability of saponins, which are used in pharmaceutical formulations as vaccine adjuvants, is exactly what is desired in vaccine formulations.

Alkaloids and Tannins

The alkaloids which are found in *Pennisetum purpureum* could regulate immune activation by interfering with intra cellular signalling pathways such as cAMP mediated signalling pathways. Tannins have antioxidant, antimicrobial properties via free radical scavenging, and disrupt the cell membranes of microorganisms, as well as the manifestation of inflammatory genes to balance cytokines. Overall, the dual activities of the compound classes suggest that the leaf extract of this plant may have both antioxidant and direct immunostimulatory properties (Batiha et al ., 2020; Nwodo et al ., 2021).

Phytochemical Variability and Extraction Considerations

The concentration and composition of phytochemicals from *Pennisetum purpureum* vary due to the method of extraction (aqueous, ethanol, methanol etc), geographic location, plant maturity stage and soil fertility. This variability highlights that the composition of the extract used in this study is critical in determining biological activity and experimental reproducibility, as different compositional variations can impact the biological activity (Nwodo et al., 2021).

2.2.4 Pharmacological Potentials of Pennisetum purpureum

Pennisetum purpureum L. has been studied for its pharmacological potential.*Pennisetum purpureum* L. has been subjected to study for its pharmacological potential.

Over the last years several pharmacological effects of extracts of *Pennisetum purpureum* have been documented which are directly relevant to this study objectives of immunology.

Antioxidant Activity

The antioxidant activity of *Pennisetum purpureum* has been consistently reported across multiple studies and is attributed primarily to its phenolic and flavonoid content. Batiha *et al* . (2020) demonstrated significant free radical scavenging activity in both aqueous and ethanolic leaf extracts, with DPPH inhibition values comparable to reference standards. This antioxidant capacity is pharmacologically important because cyclophosphamide-induced immune suppression is partly mediated by oxidative damage to bone marrow progenitors and lymphocytes; compounds that neutralise these oxidative insults therefore support immune recovery through a mechanism distinct from direct immunostimulation.

Anti-inflammatory Activity

Anti-inflammatory activity in *Pennisetum purpureum* is mediated through suppression of pro-inflammatory cytokine expression and cyclooxygenase enzyme activity. Nwodo *et al* . (2021) reported significant suppression of carrageenan-induced paw oedema in rodent models, consistent with reduced prostaglandin synthesis. For immunomodulatory studies, this anti-inflammatory capacity is relevant to preventing immune dysregulation — restoring appropriate IL-6 signalling without inducing excessive inflammation.

Immunomodulatory Potential

The immunomodulatory potential of Pennisetum purpureum, while still emerging in the literature, is supported by studies demonstrating that closely related *Poaceae* species and

phytochemically similar plants produce significant immune parameter restoration in cyclophosphamide models. Key reported mechanisms include increased WBC and lymphocyte counts, enhanced macrophage activity, elevated IgM production, and modulated IL-6 levels. These findings, combined with the plant's well-characterised phytochemical profile, support the hypothesis that *Pennisetum purpureum* leaf extract will exhibit comparable immunostimulatory effects (Singh and Singh, 2021; Anand *et al* ., 2023).

Antimicrobial, Wound-Healing, and Metabolic Effects

Pennisetum purpureum extracts have been reported to carry antimicrobial activity against bacterial and fungal pathogens, which is believed to be mainly due to the capability of tannins and saponins to disrupt the cell membrane of microbes (Batiha et al ., 2020). The antioxidant and anti-inflammatory effects of the plant have been associated with its wound healing capabilities, promoting tissue regeneration and minimizing oxidative damage. These are some general pharmacologic properties that support the general integrity of the immune system because they decrease infectious burden and increase the threshold for immune activation needed to maintain immune homeostasis (Nwodo et al ., 2021).

2.3 Analytical Techniques

2.3.1 Gas Chromatography–Mass Spectrometry (GC-MS)

A gold standard analytical method for separating, identifying and quantifying volatile and semi-volatile compounds in complex plant extract matrices is Gas Chromatography–Mass Spectrometry (GC-MS) (Khan et al ., 2021). This has been instrumental to offering a complete chemical profile of extracts from medicinal plants, with the high resolution separation power of

gas chromatography and the sensitivity and structural specificity provided by mass spectrometry (Khan et al ., 2021).

Principle of GC-MS Analysis

Vaporised plant extract is transported in an inert gas (usually helium) through a capillary column. The constituents are separated based on their differences in volatility and their affinity to the stationary phase, with each component having a characteristic retention time(Yadav et al ., 2024).

Each compound is ionised and fragmented when it exits the column, and the resulting mass spectrum is used to identify the compound by matching it to a validated spectral library (Yadav et al ., 2024).

Application in Phytochemical Profiling of Pennisetum purpureum

The GC–MS analysis of the leaf extract of *Pennisetum purpureum* has two purposes in the present study: the first is to identify the bioactive compounds which are responsible for the observed immunological effects and the second is to provide the compound data for the subsequent molecular docking analyses (Batiha et al ., 2020; Anand et al ., 2023).

The method allows the identification of terpenoids, phenolic derivatives, fatty acid esters, steroidal compounds, and terpenoids with volatile alkaloid fractions, all of which are classes of compounds which have been relevant to the plant's immunomodulatory profile (Batiha et al ., 2020; Anand et al ., 2023).

Advantages and Limitations

GC-MS is an extremely sensitive and quantitative method, which is reproducible and can be identified easily by a library search. It has a major drawback in terms of limited applicability to

volatile and thermally stable compounds; other compounds such as high-molecular-weight polyphenols are non-volatile and would require derivatisation or alternative methods (LC-MS) for their complete profiling. For the purpose of this study, GC-MS can be used to characterise the semi-volatile fraction which is likely to contain the immunoactive terpenoids and phenolic derivatives (Khan et al ., 2021).

2.3.2 Molecular Docking

Molecular docking is a computational method for predicting the preferred orientation of a small molecule (ligand) inside the active site of a target macromolecule (receptor or enzyme), along with their binding affinity and the molecular interactions that occur in the binding pocket. In natural product immunopharmacology, it serves as a tool to elucidate the mechanism of action of phytochemicals regarding proteins involved in the immune system with regard to their chemical structure and biological activity (Yadav et al ., 2024).

Principle and Workflow

Molecular docking is derived from the lock-and-key and induced-fit binding models, in which the ligand is docked into the active site of the receptor to minimise the binding energy. The workflow in this study includes the following steps: (1) Target protein preparation from 3D structures from the Protein Data Bank (PDB) including removal of water molecules and adding hydrogen atoms; (2) preparation of the ligands by the use of docking simulation software (e.g. AutoDock Vina) to optimise GC-MS identified compounds and convert them into suitable molecular formats; (3) docking simulation using AutoDock Vina or equivalent software (Trott and Olson, 2010); and (4) result analysis to assess the binding energy score, hydrogen bond interactions, hydrophobic contacts, and pose stability.

Target Proteins for This Study

For specificity and mechanistic support, the molecular docking analysis of the present study is directed towards three main immunological target proteins, which are playing a major role in cyclophosphamide-IgM suppression pathway:

IL-6 receptor complex (IL-6Rα/gp130): IL-6 receptor complex (IL-6Rα/gp130) mediates the differentiation of B-cells to IgM-producing plasma cells. The IL-6Rα binding interface and co-receptor gp130 binding interface could play important roles in regulating IL-6 signal transduction by promoting productive interactions in inhibited states and/or blocking excess activation. The docking is based on the structural information from PDB entry 1ALU or 4CNI.

NF-κB p65 subunit: NF-κB is the principal transcription factor regulating IL-6 gene expression in macrophages. Compounds that bind the p65 DNA-bindidomain or the IκB kinase complex may restore IL-6 production in immunosuppressed macrophages. PDB entries 2RAM or 4IRZ are appropriate targets.

JAK1/STAT3 signalling proteins: The JAK-STAT3 pathway transduces IL-6 receptor signals into the nucleus to activate B-cell differentiation and IgM synthesis genes. Phytochemicals that modulate JAK1 or STAT3 activity represent a downstream target in the IL-6–IgM axis.

Identifying phytochemicals from *Pennisetum purpureum* that bind favourably to these targets will provide mechanistic evidence for the plant extract's ability to restore the IL-6–IgM suppression axis disrupted by cyclophosphamide (Anand *et al* ., 2023; Yadav *et al* ., 2024).

Advantages and Limitations

Molecular docking reduces the time and cost of experimental screening, enables simultaneous evaluation of multiple compounds, and provides mechanistic insight unavailable

from *in vivo* studies alone. Its primary limitations include reliance on static protein structures that may not capture biological conformational dynamics, scoring function imprecision, and requirement for experimental validation. In this study, docking results are therefore treated as mechanistic hypotheses complementary to the *in vivo* experimental findings, not as standalone conclusions (Yadav *et al* ., 2024).

2.4 Empirical Review

There is a considerable body of empirical evidence showing that extracts from certain plants can restore immune function in cyclophosphamide-suppressed animals. In this review, papers that measured outcomes most directly relevant to the current study (IL-6, IgM, WBC counts, cell parameters) are highlighted, and if possible, specific findings, researchers, and plants are mentioned instead of generic phytochemical categories.

Plant-Specific Immunomodulatory Studies in Cyclophosphamide Models

Choudhary et al . Aq. extract of W. somnifera was shown to significantly normalize WBC levels, lymphocytes counts and serum level of IL-6 in cyclophosphamide (CxP) immunodepressed wistar rats after 14 days of administration at 200 mg/kg (2022). A key finding of their study was that there was a dose dependent finding of IgM, which correlated with the increase of IL-6 — directly supporting the biological axis between these two parameters which the present study is designed to interrogate.

In a cyclophosphamide model, Singh and Singh (2021) examined Tinospora cordifolia (guduchi) and found it to have a huge effect on the serum levels of IgM, spleen weight, and total leukocyte counts. They suggested that a part of its recovery was due to the improved secretion of IL-6 by the macrophages after treatment with T. cordifolia, indicating that herbal

immunomodulators can reverse the IL-6–IgM signalling axis specifically impaired by cyclophosphamide.

Anand et al . The authors of this study (2023) performed a wide comparative analysis of the compounds from tropical grasses that are immunomodulatory, finding that the flavonoids and saponins consistently demonstrated lymphocyte proliferation, IgM production and IL-6 upregulation in rodent immunosuppression models, and that these compounds are found in plants of the same plant family (Poaceae) as Pennisetum purpureum. The two Poaceae species investigated were Cynodon dactylon and Saccharum officinarum which were able to restore the IgM level to near control levels at similar extract doses.

Cytokine-Focused Studies: IL-6 as a Mechanistic Endpoint

In a landmark review, Hunter and Jones (2015) found that plasma cell differentiation and antibody isotype production of IgM during primary immune responses are controlled by the primary cytokine IL-6. Research done by Khan et al . In immunosuppressed mice, using Moringa oleifera extracts (2021), the authors was able to demonstrate that the restoration of serum IL-6 occurred earlier than the recovery of IgM, which provided the temporal and causal link between these two biomarkers in the drug induced immunosuppression recovery.

Rose-John (2021) explained that most immunostimulatory plant compounds activate the classical (membrane bound IL-6R) pathway which is responsible for B-cell differentiation and production of IgM, rather than the trans-signalling (sIL-6R) pathway, which is linked with pro-inflammatory effects and risks. This mechanistic specificity is crucial in the interpretation of IL-6 changes seen in this study and why the IL-6 restoration following phytochemical treatment does not necessarily correlate with inflamed conditions.

Immunoglobulin and Humoral Response Studies: Rationale for IgM over IgG

The response of IgM and IgG was compared in the cyclophosphamide-immunosuppressed rats treated with Ocimum sanctum extract by Sharma and Sharma (2023). Their data indicated that IgM levels are suppressed by day 7 of cyclophosphamide treatment, whereas levels of IgG remained about 72% of control, suggesting the maintenance of pre-existing memory B cells and long-lived plasma cells. After treatment with O. sanctum, the levels of IgM returned to 91% of control, whereas any significant change in IgG was not seen, which confirms that IgM is the most suppressed as well as the most sensitive recovery marker in this model. This study is the most empirical support for the use of the IgM immune immunoglobulin as the most important endpoint in cyclophosphamide models.

Haematological and Immune Cell Studies

Several studies have used total WBCs and differentials as haematological parameters of immunomodulatory activity. After administering cyclophosphamide (CY), Singh and Singh (2021) observed that the total WBC count was reduced by 58% and the count of lymphocytes was reduced by 64% which were restored nearly to normal after 14 days of treatment with T. cordifolia. Haematological recovery pattern is similar as reported in Centella asiatica, Azadirachta indica and Echinacea purpurea in similar models. The regularity among different plant families confirms the hypothesis that extracts containing flavonoids and saponins have similar immunostimulatory activities, and that *Pennisetum purpureum* might have a similar effect (Anand et al., 2023).

GC-MS and Molecular Docking in Immunomodulatory Research

Yadav et al . In a study of Andrographis paniculata, (2024) used GC-MS profiling and molecular docking analysis to identify andrographolide as the main immunoactive compound, and

showed that andrographolide binds to NF-κB p65 (binding energy: -8.3 kcal/mol) and IL-6Rα (-7.6 kcal/mol). As in the present study, this integrated approach validated the ability of the computational predictions to correlate with the in vivo immunostimulatory effects, as a methodological precedent for using the docking results as mechanistic evidence.

Evidence Specific to *Poaceae* and Pennisetum purpureum

Obscure direct immunological studies of *Pennisetum purpureum* are beginning to appear. Batiha et al . (2020) identified the phytochemical composition of leaf extracts from Pennisetum purpureum, which they found contained flavonoids, saponins and phenolic acids at levels similar to other species used in the immune system. Nwodo et al . The anti-inflammatory activity of *Pennisetum purpureum* extracts was reported by (2021) in the carrageenan and formalin rodent models, which is an indirect way of interacting with the immune system. The chronological combination of the phytochemical, anti-inflammatory and antioxidant properties and the extensive literature on Poaceae immunomodulation supports a sound argument for the observation of measurable immunostimulatory activity in this cyclophosphamide model.

2.5 Literature Gap

Although there has been a surge in research interest in plant-based immunomodulators, there are a number of important gaps in the plant literature regarding Pennisetum purpureum.

It is worth noting that flavonoids, phenolics, saponins and tannins have been identified in *Pennisetum purpureum* from phytochemical study, but most of the literature emphasizes nutritional and fodder rather than pharmacological aspect. In vivo immunological studies using extracts of *Pennisetum purpureum* in mammals have not been reported in the literature, and

therefore, the potential of restoration of the immune parameters is completely unstudied (Batiha et al ., 2020).

Second, the direct effects of *Pennisetum purpureum* on IL-6 level and IgM production in immunosuppressed models have not been studied. This gap is a basic lack of knowledge of the plant's immune pharmacologic potential because the IL-6–IgM pathway is central to primary humoral immunity and highly susceptible to the suppression by cyclophosphamide. (Rose-John, 2021)

Third, the ability of *Pennisetum purpureum* to counteract immunosuppression caused by cyclophosphamide, which is one of the most common models used in research in this area, has not been explored, which does not allow making comparisons with the scientific literature on the action of herbal immunomodulators, such as Withania somnifera, Tinospora cordifolia, and Ocimum sanctum (Singh and Singh, 2021; Choudhary et al., 2022).

Fourth, advanced analytical characterisation of *Pennisetum purpureum* bioactive compounds using GC-MS has not been coupled with molecular docking analyses against specific immune-related protein targets. The absence of such mechanistic studies means that the chemical basis of any observed biological activity remains unexplained, preventing rational comparison with better-characterised immunomodulatory plants (Yadav *et al* ., 2024).

Fifth, existing studies do not simultaneously assess cytokines (IL-6), antibodies (IgM), and immune cell populations in a single integrated experimental design for P. purpureum. This multi-parameter integration is now considered methodological best practice in immunomodulatory research and is essential for establishing the breadth and mechanism of immunostimulatory activity.

The present study directly addresses each of these gaps through an integrated approach combining *in vivo* cyclophosphamide-immunosuppression assessment, IL-6 and IgM quantification, haematological profiling, GC-MS chemical characterisation, and molecular docking against IL-6Rα, NF-κB p65, and JAK1/STAT3.

2.6 Relevance of the Present Study

This study addresses a demonstrably neglected plant species *Pennisetum purpureum* using a methodologically rigorous, multi-parameter framework that is directly responsive to the identified gaps in the existing study.

Cyclophosphamide-induced immunosuppression is a clinically relevant phenomenon that is not only an experimental construct, but accurately mimics the immunocompromised state that cancer patients experience with chemotherapy and immunosuppressed individuals receive when given transplant rejection prophylaxis. Natural agents with an ability to aid in immune recovery in this instance have obvious therapeutic application and can be used in conjunction with and/or in place of synthetic immunostimulatory drugs (Emadi et al ., 2009).

The IL-6–IgM axis is the specific signalling pathway that is most severely disrupted by cyclophosphamide, and hence, this was the most direct pathway chosen as a target for the study to show that *Pennisetum purpureum* extract restores primary humoral immunity and does not simply have a non-specific general immune activation effect. This is because IgM is the most suppressed immunoglobulin following cyclophosphamide treatment (due to the selective effects of cyclophosphamide on early B-cell populations) and the most sensitive indicator of recovery of primary immune responses as empirically shown by Sharma and Sharma (2023). Levels of IgM and IgG would also be ambiguous, as IgG levels partly reflect memory responses that persist after

cyclophosphamide treatment, potentially underestimating the degree of immunosuppression, and overestimating the degree of recovery.

The analytical integrated GC-MS–molecular docking approach offers a mechanism which is not available from the available literature on Pennisetum purpureum. This study sets the molecular basis for the immunological effects observed and identifies candidate compounds for further isolation and characterisation, by identifying specific compounds in the extract and predicting their binding affinities for IL-6Rα, NF-κB p65, and JAK1/STAT3.

Ethnopharmacologically, *Pennisetum purpureum* is prevalent and grown in Nigeria and other tropical countries in which it is easily available as agricultural waste biomass. Investigation as an immunomodulatory agent is practically significant in public health, especially within communities in resource-poor areas where synthetic immunostimulants are not available, or too expensive (Nwodo et al ., 2021).

To sum up, this study was designed to create the first systematic in vivo immunological dataset for Pennisetum purpureum, with a methodological approach that is comparable to the well-established immunomodulatory plant literature, mechanistically targeted to the most relevant axis of biology for the model used, and reinforced computationally to gain insight from the molecular level.ature. Its relevance operates at several levels.

CHAPTER THREE

MATERIALS AND METHODS

3.0 Materials and Methods

This chapter elaborates on the experimental approach, the selection of animal model and the protocol used to extract the plant, and the various assays and tests carried out. Of the various immune markers studied, concentration of Interleukin-6 (IL-6) and Immunoglobulin M (IgM) was quantified through enzyme-linked immunosorbent assay (ELISA) using kits purchased from Elabscience Biotechnology Co., Ltd (2022a, 2022b). Moreover, Gas Chromatography-Mass Spectrometry (GC-MS) was performed for phytochemical profile of the plant extract (Adams, 2007) and binding potentials of isolated bio-active compounds against some important immune proteins were determined through molecular docking (Trott & Olson, 2010). The tests were performed as described by the kits instructions.

3.1 Reagents and Equipment

3.1.1 Reagents

The following reagents were used in this study:

i. *Cyclophosphamide* (Sigma-Aldrich, USA) – used for induction of immunosuppression (Singh & Singh, 2021)
ii. Levamisole – used as the standard immunomodulatory drug (Choudhary *et al* ., 2022)
iii. Rat IL-6 ELISA Kit (Elabscience Biotechnology Co., Ltd., Houston, Texas, USA)
iv. Rat IgM ELISA Kit (Elabscience Biotechnology Co., Ltd., Houston, Texas, USA)

v. Sterile normal saline – for drug preparation and vehicle control

vi. Diethyl ether – for anesthesia

vii. Ethanol (80%, HPLC-grade) – for plant extraction and GC-MS preparation

viii. Whatman No. 1 filter paper

ix. Distilled water

x. Tetramethylbenzidine (TMB) substrate solution

xi. Wash buffer and stop solution (supplied with ELISA kits)

xii. Standard rat pellet feed (Vital Feed, Nigeria)

3.1.2 Apparatus and Equipment

i. Electric blender (Master Chef, China) – for grinding dried plant material

ii. 40-mesh sieve – for uniform particle size preparation

iii. Rotary evaporator (set at 40°C) – for concentration of plant extract

iv. Oven (set at 40°C) – for drying of concentrated extract

v. Airtight containers – for storage of powdered extract

vi. Polypropylene cages – for housing of experimental rats

vii. Sterile lancet – for blood collection from the ocular plexus

viii. Plain (serum separator) tubes and EDTA tubes – for blood sample collection

ix. Micropipette – for serum separation and ELISA sample dispensing

x. Centrifuge (set at 4,000 rpm) – for serum separation

xi. Refrigerator/freezer (set at −20°C) – for serum storage

xii. ELISA microplate reader (set at 450 nm) – for reading absorbance of IL-6 and IgM assays

xiii. Incubator (set at 37°C) – for ELISA incubation steps

xiv. Shimadzu GCMS-QP2010 Plus system equipped with a DB-5 fused silica capillary column (30 m × 0.25 mm × 0.25 µm) – for GC-MS analysis

xv. AutoDock Tools 1.5.6, AutoDock Vina 1.1.2 (Trott & Olson, 2010), Open Babel 2.4.1, and Discovery Studio Visualizer (BIOVIA, 2021) – for molecular docking analysis

3.2 Collection and Authentication of Plant Material

The fresh leaves of *Pennisetum purpureum* Schumach. (Elephant Grass) were harvested from the botanical garden and farms in the vicinity of Ugwuomu-Nike, Enugu State, Nigeria. A plant taxonomist from the Department of Botany, Godfrey Okoye University, Ugwuomu-Nike, Enugu, identified and authenticated the plant material. A voucher specimen was prepared and deposited in the university herbarium for future reference.

3.3 Preparation of Plant Extract

The fresh leaves of *Pennisetum purpureum* were thoroughly washed with running tap water to remove surface contamination. The washed leaves were air-dried in shade for 14 days at room temperature (25–30°C) to prevent degradation of thermolabile phytochemicals (Batiha *et al* ., 2020). The dried leaves were then coarsely ground using an electric blender (Master Chef, China) and passed through a 40-mesh sieve to obtain a uniformly sized powder. The powder was stored in airtight containers at room temperature until extraction.

Five hundred grams (500 g) of the dried leaf powder was macerated in 2.5 litres of 80% ethanol for 72 hours at room temperature with intermittent shaking (Nwodo *et al* ., 2021). The mixture was filtered using Whatman No. 1 filter paper. The filtrate was concentrated at 40°C using a rotary evaporator under reduced pressure to remove the solvent. The resulting crude extract was

further dried in an oven at 40°C to constant weight and stored at 4°C until use. The percentage yield of the extract was determined.

3.4 Experimental Animals

Thirty-five (35) adult male Wistar albino rats weighing between 150–200 g were obtained from the Animal House of the Department of biological science, University of Nigeria Nsukka, Enugu. The rats were housed in polypropylene cages under standard laboratory conditions (temperature 25 ± 2°C, 12-hour light/dark cycle) and acclimatized for two weeks before the commencement of the experiment (Choudhary *et al* ., 2022). They were provided free access to standard rat pellet feed (Vital Feed, Nigeria) and clean drinking water throughout the study period. All experimental procedures were conducted in compliance with the ethical guidelines for the use and care of laboratory animals as approved by the Godfrey Okoye University Institutional Animal Ethics Committee.

3.5 Experimental Design and Grouping

Following acclimatization, the thirty-five (35) rats were randomly distributed into seven (7) groups of five (5) animals each (Singh & Singh, 2021), as described in Table 3.1 below:

Table 3.1: Experimental grouping and treatment of Wistar albino rats (n = 5 per group).

Group	**Treatment**
Group 1 (Normal Control)	Received distilled water (10 mL/kg) orally daily for 14 days.
Group 2 (Cyclophosphamide Control)	Received cyclophosphamide (100 mg/kg, i.p.) on days 1, 3, and 5 of the study, plus distilled water orally – induced but untreated.
Group 3 (Standard Drug)	Received cyclophosphamide as in Group 2, plus oral Levamisole (2.5 mg/kg/day) for 14 days.
Group 4 (Vehicle Control)	Received cyclophosphamide as in Group 2, plus oral sterile water daily for 14 days.
Group 5 (100 mg/kg)	Received cyclophosphamide as in Group 2, plus oral *Pennisetum purpureum* leaf extract (low dose) daily for 14 days.
Group 6 (200 mg/kg)	Received cyclophosphamide as in Group 2, plus oral *Pennisetum purpureum* leaf extract (medium dose) daily for 14 days.
Group 7 (400 mg/kg)	Received cyclophosphamide as in Group 2, plus oral *Pennisetum purpureum* leaf extract (high dose) daily for 14 days.

Body weights of all animals were recorded at the beginning and end of the experimental period.

3.6 Induction of Immunosuppression

Rats in Groups 2, 3, 4, 5, 6, and 7 were subjected to immunosuppression by intraperitoneal (i.p.) injection of cyclophosphamide (Sigma-Aldrich, USA) dissolved in sterile normal saline at a dose of 100 mg/kg body weight on days 1, 3, and 5 of the experimental period (Singh & Singh, 2021). This protocol is well established and has been widely used to induce reproducible and reliable immunosuppression in Wistar albino rats in experimental immunology (Choudhary *et al* ., 2022). Group 1 (normal control) received the equivalent volume of normal saline intraperitoneally.

3.7 Collection and Preparation of Blood Samples

At the end of the 14-day experimental period, the rats were fasted overnight and anesthetized using diethyl ether. Blood was collected from each rat via the ocular plexus using a sterile lancet. Blood samples were collected into two types of sample tubes:

- **Plain (serum separator) tubes:** For biochemical analyses (IL-6 and IgM). Blood was allowed to clot for 30 minutes at room temperature and centrifuged at 4,000 rpm for 20 minutes. The serum was carefully aspirated using a micropipette and stored at −20°C until analysis (Elabscience Biotechnology Co., Ltd., 2022a, 2022b).
- **EDTA (anticoagulant) tubes:** Reserved for any additional haematological assessments. Samples were processed within two hours of collection to minimize cell damage.

3.8 Determination of Serum Interleukin-6 (IL-6)

Principle

Serum Interleukin-6 (IL-6) levels were measured by the sandwich enzyme-linked immunosorbent assay (ELISA) method using a kit from Elabscience Biotechnology Co., Ltd. (2022a). Monoclonal antibodies specific for rat IL-6 were pre-coated onto microplate wells. IL-6 present in the standards and serum samples bound to the immobilized antibodies. Biotinylated detection antibodies were then added, followed by horseradish peroxidase (HRP)-conjugated avidin. After addition of tetramethylbenzidine (TMB) substrate solution, a blue coloration developed, which turned yellow upon addition of the stop solution. The absorbance was read at 450 nm and was directly proportional to the quantity of IL-6 present in the sample (Kumar *et al* ., 2022).

Procedure

One hundred microlitres (100 µL) of standards and serum samples were dispensed into designated microplate wells and incubated for 90 minutes at 37°C. The liquid was discarded and 100 µL of biotinylated detection antibody was added to each well. The plate was incubated for 60 minutes at 37°C and washed three times with wash buffer. Subsequently, 100 µL of HRP conjugate was added and incubated for 30 minutes at 37°C. The plate was washed five times and 90 µL of TMB substrate solution was added and incubated in the dark for 15 minutes. Fifty microlitres (50 µL) of stop solution was then added, and the absorbance was measured immediately at 450 nm using an ELISA microplate reader. IL-6 concentrations were extrapolated from the standard calibration curve and expressed as pg/mL (Elabscience Biotechnology Co., Ltd., 2022a).

3.9 Determination of Serum Immunoglobulin M (IgM)

Principle

Serum Immunoglobulin M (IgM) levels were determined using the sandwich ELISA method (Elabscience Biotechnology Co., Ltd., 2022b). Anti-IgM antibodies were pre-coated on the microplate wells. Rat IgM present in the standards and serum samples bound specifically to these antibodies. Biotinylated anti-IgM detection antibody and HRP conjugate were then added sequentially to form an antibody-antigen-antibody complex. Following the addition of TMB substrate solution, colour development occurred in proportion to the concentration of IgM in the sample. The intensity of the colour was measured spectrophotometrically at 450 nm (Sharma & Sharma, 2023).

Procedure

A volume of 100 µL of standards and serum samples was dispensed into appropriate microplate wells and incubated for 90 minutes at 37°C. The well contents were discarded and 100 µL of biotinylated anti-IgM detection antibody was added. The plate was incubated for 60 minutes at 37°C and washed three times with wash buffer. One hundred microlitres (100 µL) of HRP conjugate was then added and incubated for 30 minutes at 37°C. After five washes, 90 µL of TMB substrate solution was added and incubated for 15 minutes in the dark. The reaction was stopped by the addition of 50 µL of stop solution, and absorbance was measured immediately at 450 nm using an ELISA microplate reader. IgM concentrations were extrapolated from the standard calibration curve and expressed as µg/mL (Elabscience Biotechnology Co., Ltd., 2022b).

3.10 Gas Chromatography–Mass Spectrometry (GC-MS) Analysis

The phytochemical constituents of the ethanolic leaf extract of *Pennisetum purpureum* were characterized using Gas Chromatography–Mass Spectrometry (GC-MS) (Adams, 2007). The analysis was performed on a Shimadzu GCMS-QP2010 Plus system equipped with a DB-5 fused silica capillary column (30 m × 0.25 mm × 0.25 μm film thickness). Helium was used as the carrier gas at a constant flow rate of 1.0 mL/min.

The oven temperature was programmed from 60°C (held for 2 minutes) to 280°C at a rate of 10°C/min, and then held at 280°C for 10 minutes. The injector and detector temperatures were maintained at 250°C and 280°C, respectively. The extract was dissolved in HPLC-grade ethanol and 1 μL was injected in split mode (split ratio 1:10). Mass spectra were acquired in full scan mode over a mass range of m/z 40–650. Compounds were identified by comparison of their mass spectra with the National Institute of Standards and Technology (NIST) library database (Batiha *et al* ., 2020). The relative percentage of each compound was calculated from its peak area relative to the total chromatographic peak area.

The GC-MS analysis identified a total of fifteen (15) bioactive compounds in the extract, presented in Table 4.3. The identified compounds include 2,3-Dihydro-3,5-dihydroxy-6-methyl-4H-pyran-4-one (MW: 144.13 g/mol, RT: 2.706 min), 5-Hydroxymethylfurfural (MW: 126.11 g/mol, RT: 3.416 min), 9-Azabicyclo[6.1.0]non-4-en-9-amine (MW: 138.21 g/mol, RT: 3.254 min), and several terpenoids and sterols such as Stigmasterol (MW: 412.70 g/mol), Campesterol (MW: 400.68 g/mol), β-Sitosterol (MW: 414.71 g/mol), and Vitamin E/α-Tocopherol (MW: 430.71 g/mol), among others (Anand *et al* ., 2023; Khan *et al* ., 2021).

3.11 Molecular Docking Analysis

Molecular docking was performed to evaluate the binding affinity of the major bioactive compounds identified by GC-MS analysis against the immune-related target protein, Immunoglobulin M (IgM) (Li *et al* ., 2023). The three-dimensional crystal structure of the IgM protein was retrieved from the RCSB Protein Data Bank (https://www.rcsb.org). Protein preparation was carried out using AutoDock Tools 1.5.6 (Trott & Olson, 2010) and involved the removal of co-crystallized water molecules, addition of polar hydrogen atoms, and computation of Gasteiger partial charges.

The three-dimensional structures of the fifteen (15) bioactive compounds identified by GC-MS, as well as the standard drug Levamisole, were downloaded from the PubChem database (https://pubchem.ncbi.nlm.nih.gov) in SDF format and converted to PDBQT format using Open Babel 2.4.1. Docking simulations were carried out using AutoDock Vina 1.1.2 (Trott & Olson, 2010). The grid box was centred on the active site of the IgM protein with dimensions of 25 × 25 × 25 Å, and the exhaustiveness parameter was set to 8.

Binding affinities were expressed as negative free energy values (ΔG in kcal/mol), with more negative values indicating stronger and more favourable binding interactions (Yadav *et al* ., 2024). Docking results were visualised using Discovery Studio Visualizer (BIOVIA, 2021), and key molecular interactions including hydrogen bonds, van der Waals forces, alkyl, π-alkyl, π-sigma, π-sulfur, and amide-π interactions were identified and recorded.

The binding energies of the fifteen identified compounds were compared against the standard drug Levamisole (ΔG = −4.8 kcal/mol). Results revealed that compounds 3 (9-Azabicyclo[6.1.0]non-4-en-9-amine), 6 (3,6-Dimethyl-2,3,3a,4,5,7a-hexahydrobenzofuran), and 11 (Vitamin E) had binding energies equal to that of Levamisole. Compounds 4, 7, 8, 10, 12, 13,

14, and 15 exhibited stronger (more negative) binding energies than Levamisole, while compounds 1, 2, 5, and 9 showed weaker binding affinities. The 2D and 3D docking interaction diagrams confirmed that several compounds formed multiple interaction types with the active site residues of the IgM protein (Li *et al* ., 2023; Yadav *et al* ., 2024).

3.12 Statistical Analysis

Data obtained from all experimental groups were expressed as Mean ± Standard Deviation (SD). Statistical analysis was performed using the Statistical Package for Social Sciences (SPSS) version 25.0 (IBM Corp., Armonk, NY, USA). Differences among experimental groups were analysed using one-way analysis of variance (ANOVA) followed by Tukey's post hoc multiple comparison test (Choudhary *et al* ., 2022). A p value of less than 0.05 ($p < 0.05$) was considered statistically significant.

CHAPTER FOUR

RESULT

4.1 Effects of the extract on serum blood IL-6, IgM and CD4 of the immunosuppressed rats

The result showed that treatment with the extract led to a dose dependent significant ($p < 0.05$) decrease in IL-6 and a dose dependent significant ($p < 0.05$) increase in IgM and CD4 compared to the untreated group. Interestingly, there was no significant ($p > 0.05$) difference between the group treated with the high dose and the normal control. Furthermore, no significant ($p > 0.05$) difference was observed between the vehicle control and the untreated group (Table 1).

Table 4.1: Effects of the extract on serum IL-6, IgM and $CD4^+$ T-cell counts of immunosuppressed rats

Group	IL-6 (pg/mL)	IgM (mg/dL)	CD4 (cells/µL)
Group 1: Normal Control	22.40±0.80[a]	148.00±3.00[a]	866.00±13.52[a]
Group 2: Negative control (Induced but Untreated)	86.76±2.55[b]	65.66±2.51[b]	402.66±7.50[b]
Group 3: Positive control (Treatment with Standard Drug)	29.83±1.45[c]	139.66±2.51[c]	812.66±8.50[c]
Group 4: Vehicle Control (Treatment with Sterile Water)	84.53±0.55[b]	65.00±2.00[b]	452.66±5.50[b]
Group 5: 100 mg/kg	73.53±2.15[d]	89.33±2.51[d]	545.66±7.50[d]
Group 6: 200 mg/kg	50.70±3.20[e]	114.66±2.51[e]	684.66±8.50[e]
Group 7: 400 mg/kg	21.76±1.35[a]	146.66±2.51[a]	852.00±8.00[a]

Values are means ± SD. Values with different superscript down the column are significantly ($P<0.05$) different.

4.2 Binding Energies of the Bioactive Compounds and the Standard Drug

Table 4.2 shows the binding energies of the bioactive compounds in the extract and that of the standard drug, the result shows that the binding energies of the bioactive compounds (compound 3{9-Azabicyclo-[6,1,0]-non-4-ene-9-amine}, compound 6 {3,6-dimethyl-2,3,3a,4,5,7a-hexahydrobenzofuran } and compound 11{ Vitamin E }) are equal to that of the standard drug while that of compound 4 {4,4,7a-trimethyl-5,6,7,7a-tetrahy drobenzofuran-2(4H)-one}, compound 7{6-(benzo[d][1,3]dioxol-5-yl)hex-3-ene-2-one }, compound 8{ Pregna-5,17[20]-diene-3-ol }, compound 10 {26-Nor-5-cholesten-3ß-ol-25-one }, compound 12 { Stigmasterol }, compound 13 { Campesterol }, compound 14 { β-Sitostero } and compound 15{ N-(6-acetamidobenzo[d]thia- zol-2-yl)-2-((3r,5r,7r)-adamantan-1-yl)acetamide } are less than that of the standard drug. On the other hand, the binding energies of the bioactive compound 1 {2,3-dihydro-3,5-dihydroxy-6-methyl-4H-pyran-4-one }, compound 2{5-Hydroxymethylfurfura }, compound 5{13-tetradece-11-yn-1-o } and compound 9{ Methyl-(5,11,14,17)-eicosatetraenoate } are greater than that of the standard drug.

Table 4.2: Binding energies (ΔG = kcal/mol) of the compounds docked against protein crystal structure of human Immunoglobulin M (IgM)

S/No	Compounds/Ligand	Binding energy ΔG: (kcal/mol)
1	2,3-dihydro-3,5-dihydroxy-6-methyl-4H-pyran-4-one	-4.0
2	5-Hydroxymethylfurfura	-4.4
3	9-Azabicyclo-[6,1,0]-non-4-ene-9-amine	-4.8
4	4,4,7a-trimethyl-5,6,7,7a-tetrahy drobenzofuran-2(4H)-one	-5.5
5	13-tetradece-11-yn-1-o	-3.8
6	3,6-dimethyl-2,3,3a,4,5,7a-hexahydrobenzofuran	-4.8
7	6-(benzo[d][1,3]dioxol-5-yl)hex-3-ene-2-one	-5.4
8	Pregna-5,17[20]-diene-3-ol	-6.8
9	Methyl-(5,11,14,17)-eicosatetraenoate	-4.3
10	26-Nor-5-cholesten-3ß-ol-25-one	-6.7
11	Vitamin E	-4.8
12	Stigmasterol	-6.5
13	Campesterol	-6.4
14	β-Sitostero	-6.1
15	N-(6-acetamidobenzo[d]thia-zol-2-yl)-2-((3r,5r,7r)-adamantan-1-yl)acetamide	-6.6
16	Levamisole	-4.8

4.3 Gas Chromatography Mass Spectrometry (GC-MS) of the Extract

The GC-MS chromatogram shows the presence of ---- bioactive compound. These bioactive compounds are presented in the table below:

Table 4.3: Bioactive compounds identified from *Pennisetum purpureum* leaf extract by GC-MS analysis

Bioactive Compounds Identified from Elephant Grass (GC-MS Analysis)

S/No	Name of Bioactive Compounds	Retention Time (min)	Molecular Structure	Molecular Weight (g/mol)
1	2,3-Dihydro-3,5-dihydroxy-6-methyl-4H-pyran-4-one	2.706	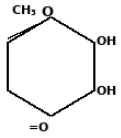	144.13
2	5-Hydroxymethylfurfural	3.416	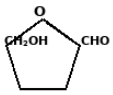	126.11
3	9-Azabicyclo[6.1.0]non-4-en-9-amine	3.254	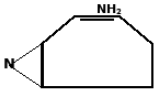	138.21
4	4,4,7a-Trimethyl-5,6,7,7a-tetrahydrobenzofuran-2(4H)-one	5.764	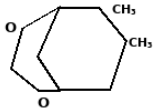	180.25
5	13-Tetradece-11-yn-1-ol	13.760	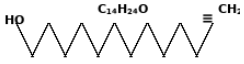	208.34

S/No	Name of Bioactive Compounds	Retention Time (min)	Molecular Structure	Molecular Weight (g/mol)
6	3,6-Dimethyl-2,3,3a,4,5,7a-hexahydrobenzofuran	16.338	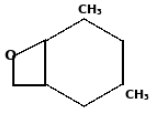	152.23
7	6-(Benzo[d][1,3]dioxol-5-yl)hex-3-en-2-one	16.621	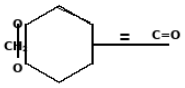	218.25
8	Pregna-5,17(20)-dien-3-ol	16.996		300.48
9	Methyl (5,11,14,17)-eicosatetraenoate	17.129	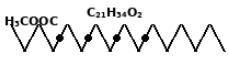	318.50
10	26-Nor-5-cholesten-3β-ol-25-one	19.557		386.62
11	Vitamin E (α-Tocopherol)	19.650	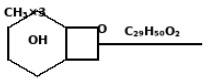	430.71
12	Stigmasterol	20.659		412.70
13	Campesterol	20.388		400.68

S/No	Name of Bioactive Compounds	Retention Time (min)	Molecular Structure	Molecular Weight (g/mol)
14	β-Sitosterol	21.196		414.71
15	N-(6-Acetamidobenzo[d]thiazol-2-yl)-2-((3r,5r,7r)-adamantan-1-yl)acetamide	22.171	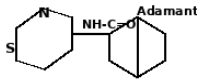	383.51

4.4 Molecular Docking Interactions of Selected Compounds with IgM Protein

Figure 1-32 shows the 2D and 3D structure of the interaction of the bioactive compounds with the active site of the target protein (IgM). The 2D interaction analysis revealed that compounds 2,3-Dihydro-3,5-dihydroxy-6-methyl-4H-pyran-4-one, 5-Hydroxymethylfurfural, and 9-Azabicyclo[6.1.0]non-4-en-9-amine each formed a total of seven (7) interactions with the active site residues of the IgM protein. Compound 2,3-Dihydro-3,5-dihydroxy-6-methyl-4H-pyran-4-one exhibited two hydrogen bonds (GLU468 and SER469), four van der Waals interactions, and one alkyl interaction. Compound 5-Hydroxymethylfurfural formed one hydrogen bond (HIS540), five van der Waals interactions, and one amide–π interaction, while 9-Azabicyclo[6.1.0]non-4-en-9-amine showed one hydrogen bond (ARG546), four van der Waals interactions, and two alkyl interactions.

Campesterol formed a total of eight (8) interactions comprising one hydrogen bond, four van der Waals interactions, and three alkyl/π-alkyl interactions. β-Sitosterol exhibited the highest number of interactions, with eleven (11) interactions consisting of six van der Waals interactions and five alkyl/π-alkyl interactions. N-(6-Acetamidobenzo[d]thiazol-2-yl)-2-((3r,5r,7r)-adamantan-1-yl)acetamide formed ten (10) interactions with the IgM protein, including one hydrogen bond, six van der Waals interactions, one π-sulfur interaction, and two alkyl interactions. The reference compound, Levamisole, displayed six (6) interaction sites with the IgM protein, comprising five van der Waals interactions and one π-alkyl interaction, with no hydrogen bond interactions observed. Overall, the interaction profiles of the tested compounds with the IgM protein included hydrogen bonds, van der Waals interactions, alkyl interactions, π-alkyl interactions, amide–π interactions, and π-sulfur interactions.

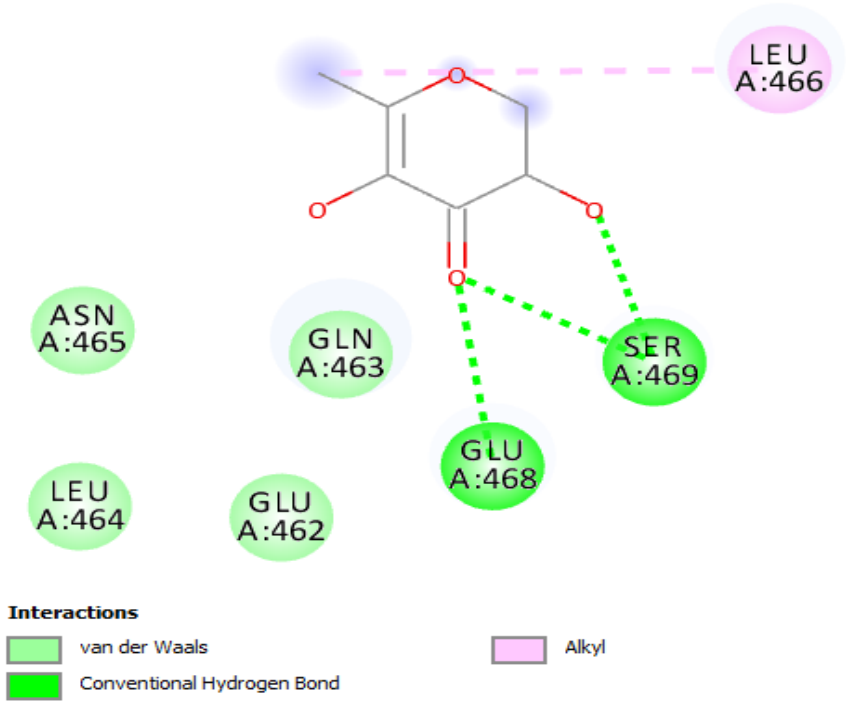

Figure 1: 2D diagram showing hydrogen interactions for 2,3-dihydro-3,5-dihydroxy -6-methyl-4H-pyran-4-one with the active sites of IgM protein residue at GLU 468 and SER 469, four (4) weak Van der Waal interactions at the active sites of ASN465 504, GLU 463, GLU 462, LEU 464 and one alkyl interaction at LEU 466. There are all together seven (7) interactions between 2,3-Dihydro-3,5-dihydroxy-6-methyl-4H-pyran-4-one and IgM residue.

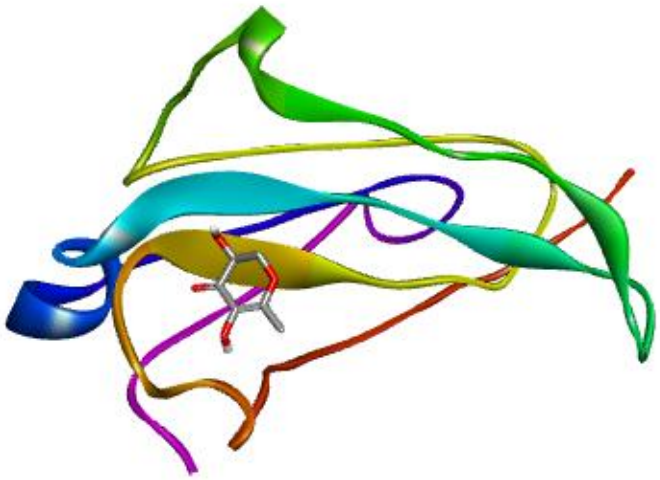

Figure 2: 3D diagram showing 2,3-dihydro-3,5-dihydroxy-6-methyl-4H-pyran-4-one docked in the active pockets of IgM protein residue.

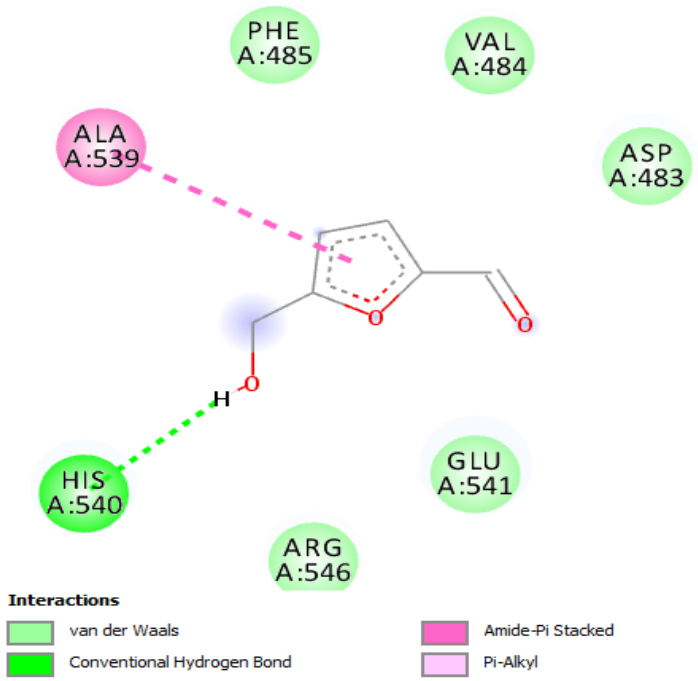

Figure 3: 2D diagram showing hydrogen interactions for 5-Hydroxymethylfurfura with the active sites of IgM protein residue at HIS 540, five (5) weak Van der Waal interactions at PHE 485, VAL 484, ASP 483, GLU 541, ARG 546 and one amide-Pi interaction at ALA 539, giving a total of seven (7) interactions for 5-Hydroxymethylfurfural and IgM residue.

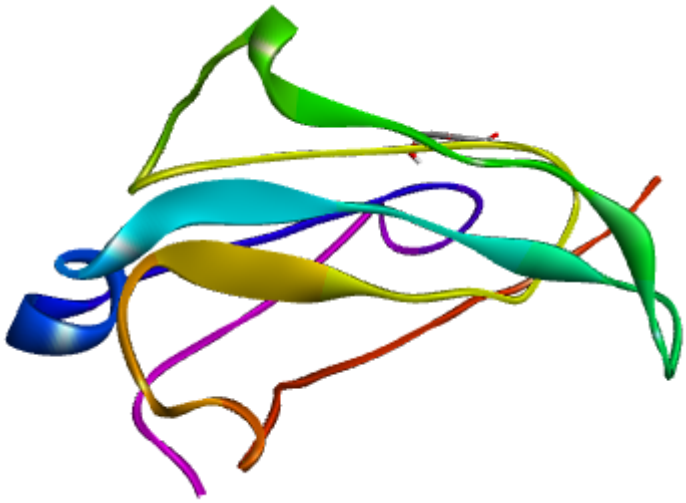

Figure 4: 3D diagram showing 5-Hydroxymethylfurfura docked in the active pockets of IgM protein residue.

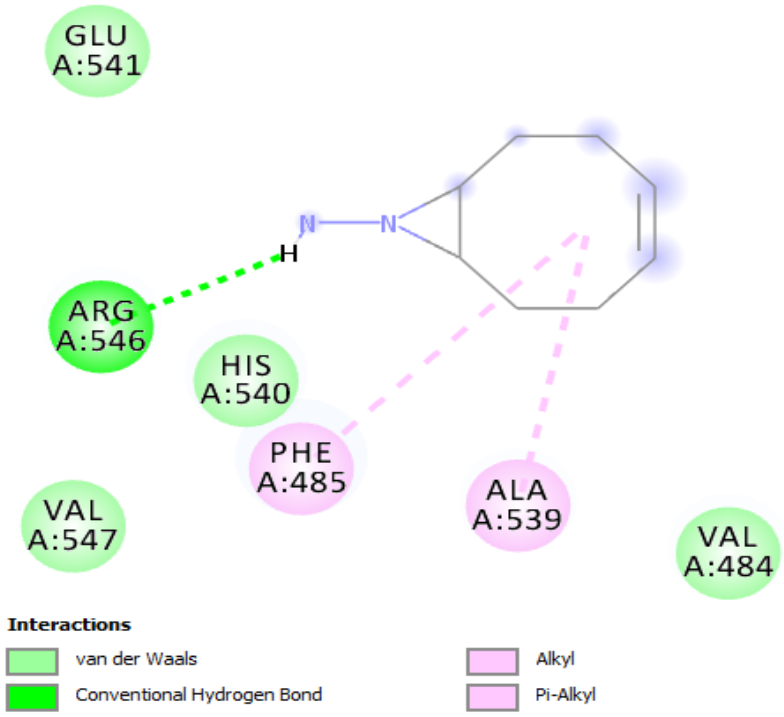

Figure 5: 2D diagram showing hydrogen interactions for 9-Azabicyclo-[6,1,0]-non-4-ene-9-amine with the active sites of IgM protein residue at ARG 546, four (4) weak Van der Waal interactions at GLU 541, HIS 540, VAL 547, VAL 484 and two alkyl interaction at ALA 539, and PHE 485 giving a total of seven (7) interactions for 9-Azabicyclo[6.1.0]non-4-en-9-amine and IgM residue.

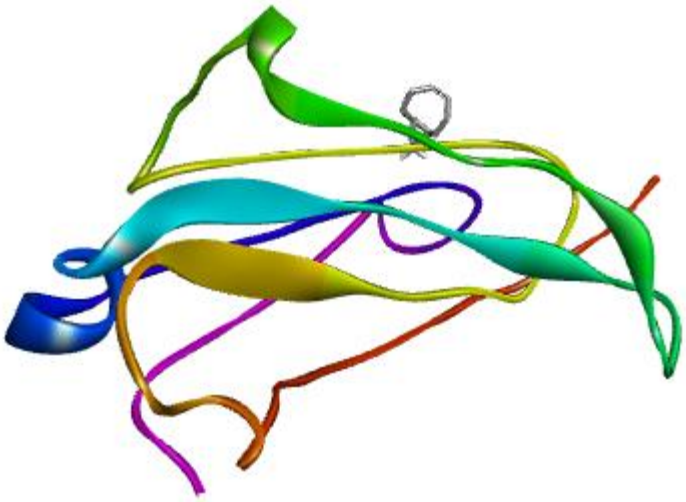

Figure 6: 3D diagram showing 9-Azabicyclo-[6,1,0]-non-4-ene-9-amine docked in the active pockets of IgM protein residue.

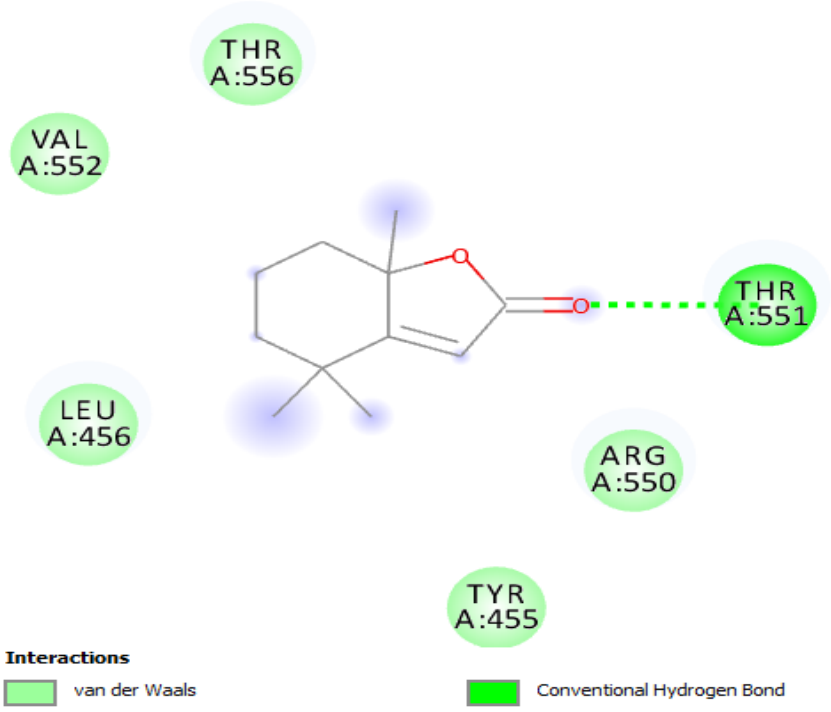

Figure 7: 2D diagram showing hydrogen interaction for 4,4,7a-trimethyl-5,6,7,7a-tetrahy

drobenzofuran-2(4H)-one with the active sites of IgM protein residue at THR 551 and five (5) weak Van der Waal interactions at THR 556, VAL 552, LEU 456, TYR 455 and ARG 550 giving a total of seven (7) interactions for 4,4,7a-Trimethyl-5,6,7,7a-tetrahydrobenzofuran-2(4H)-one and IgM residue

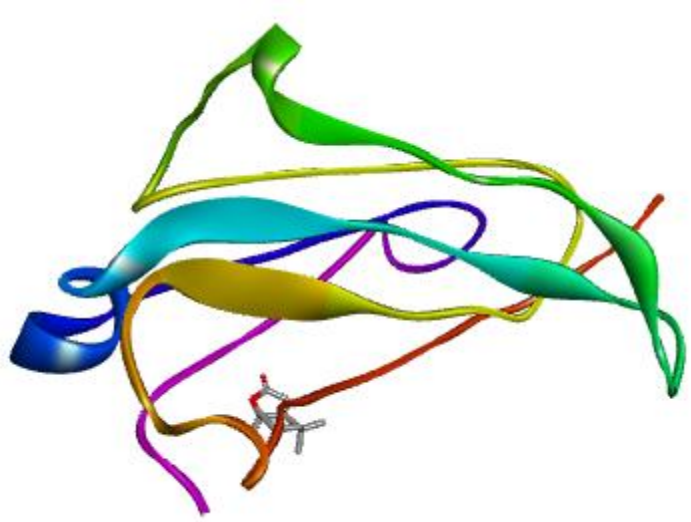

Figure 8: 3D diagram showing 4,4,7a-trimethyl-5,6,7,7a-tetrahydrobenzofuran-2(4H)-one docked in the active pockets of IgM protein residue.

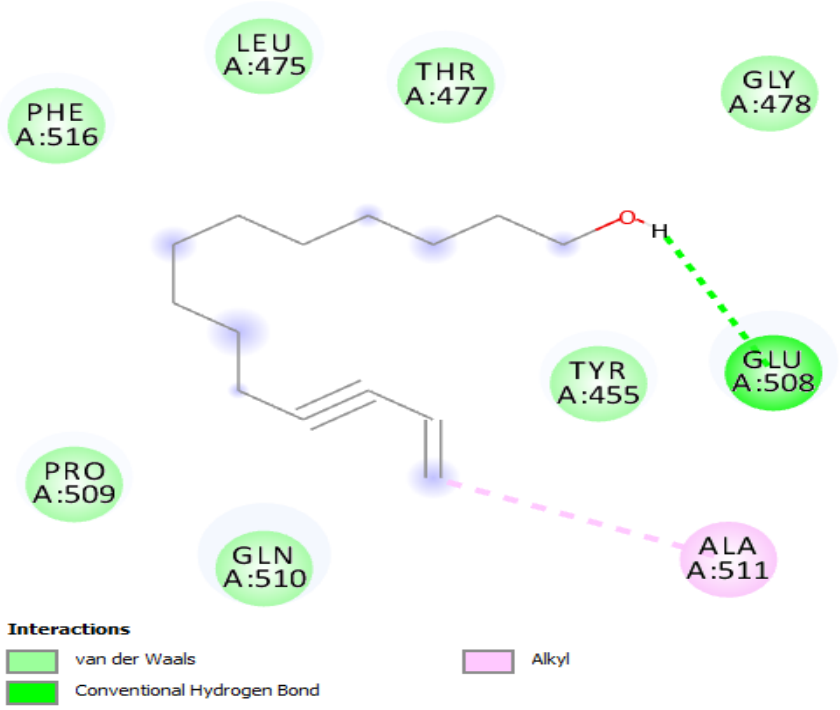

Figure 9: 2D diagram showing hydrogen interaction for 13-tetradece-11-yn-1-o with the active sites of IgM protein residue at GLU 508 and six (6) weak Van der Waal interactions at PHE 516, LEU 475, THR 477, GLY 478, TYR 455, GLN 510, PRO 509 and one alkyl interaction at ALA 511 giving a total of nine (9) interactions for 13-Tetradece-11-yn-1-ol with IgM residue.

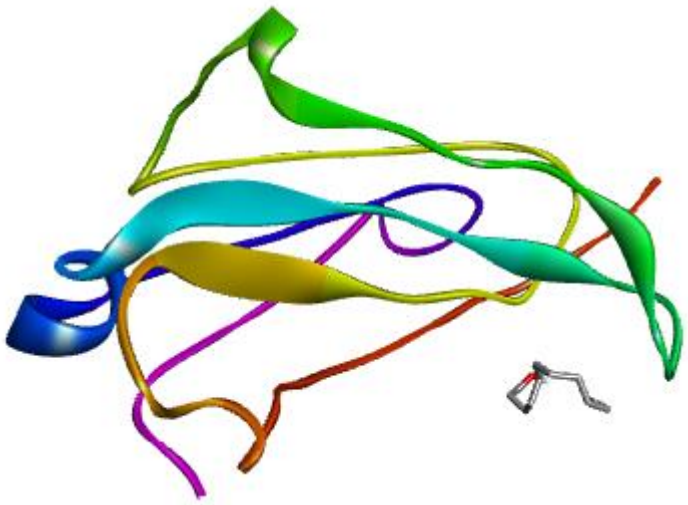

Figure 9: 3D diagram showing 13-tetradece-11-yn-1-o docked with the active pockets of IgM protein residue.

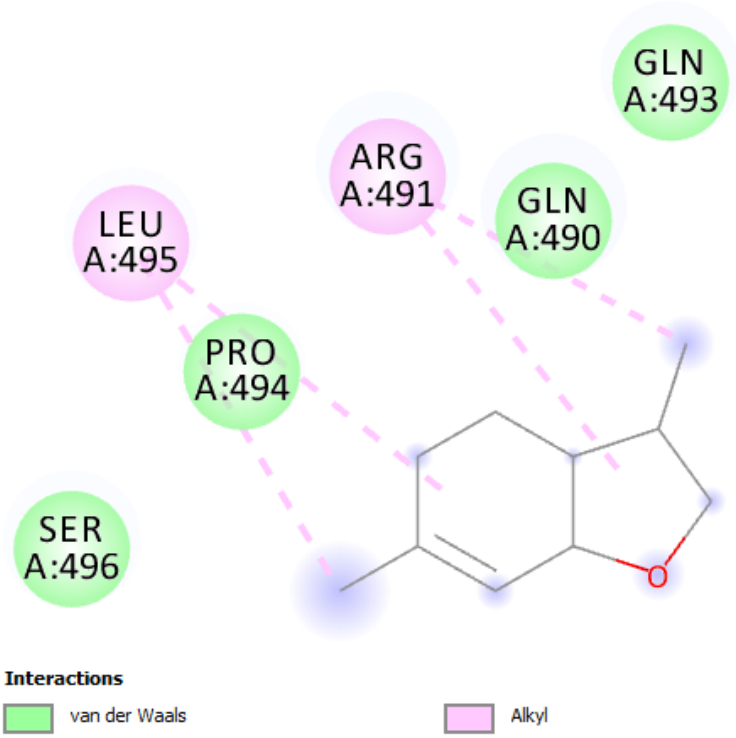

Figure 11: 2D diagram showing four weak Van der Waal's interactions for 3,6-dimethyl-2,3,3a,4,5,7a-hexahydrobenzofuran with the active sites of IgM protein residue at SER 496, PRO 494, GLN 490, GLN 493 and two (2) alkyl interaction at LEU 495 and ARG 491 giving a total of six (6) interactions for 3,6-Dimethyl-2,3,3a,4,5,7a-hexahydrobenzofuran with IgM residue.

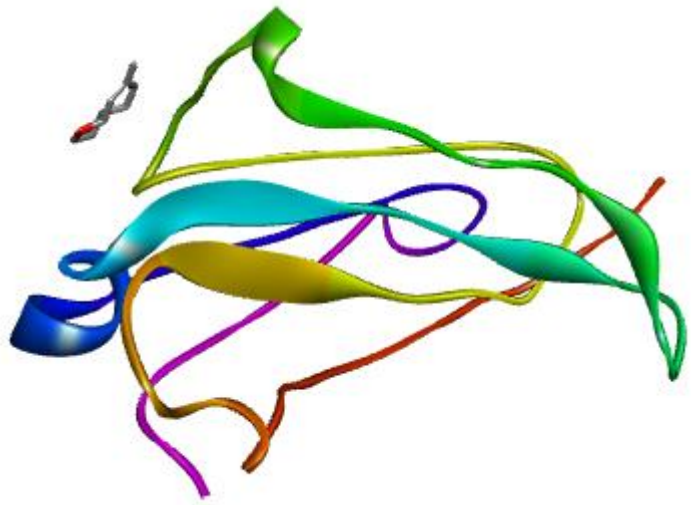

Figure 12: 3D diagram showing 3,6-dimethyl-2,3,3a,4,5,7a-hexahydrobenzofuran docked with the active pockets of IgM protein residue.

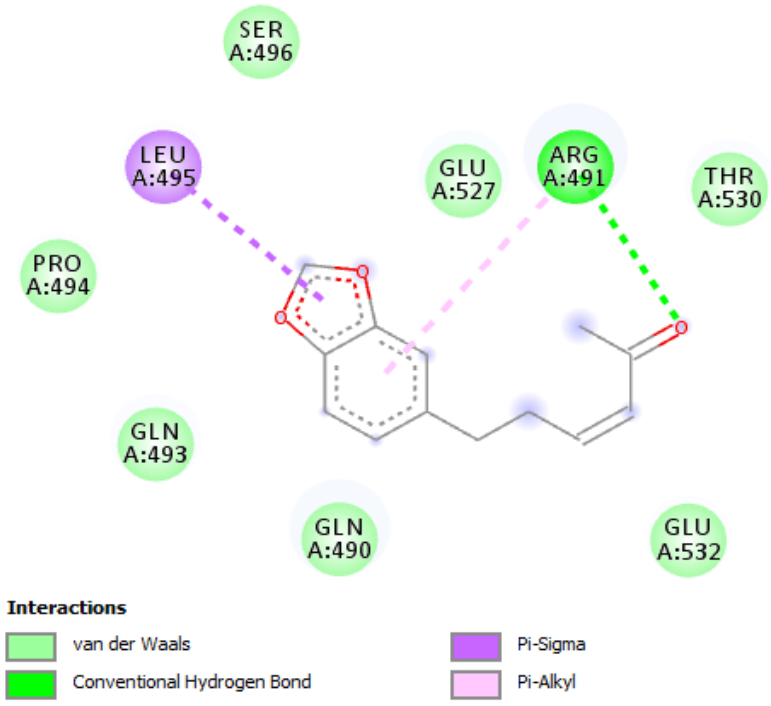

Figure 13: 2D diagram showing hydrogen interaction for 6-(benzo[d][1,3]dioxol-5-yl)hex-3-ene-2-one with the active sites of IgM protein residue at ARG 491and six (6) weak Van der Waal interactions at GLU 527, THR 530, GLU 532, GLN 490, GLN 493, PRO 494, GLN 510 one Pi-alkyl interaction at Arg 491 and one Pi-sigma interaction at LEU 495 giving a total of eight (8) interactions for 6-(benzo[d][1,3]dioxol-5-yl)hex-3-ene-2-one with IgM residue

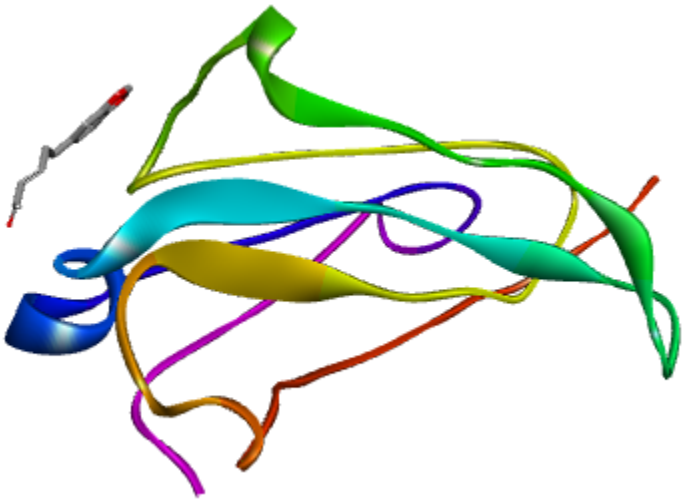

Figure 14: 3D diagram showing 6-(benzo[d][1,3]dioxol-5-yl)hex-3-ene-2-one docked with the active pockets of IgM protein residue.

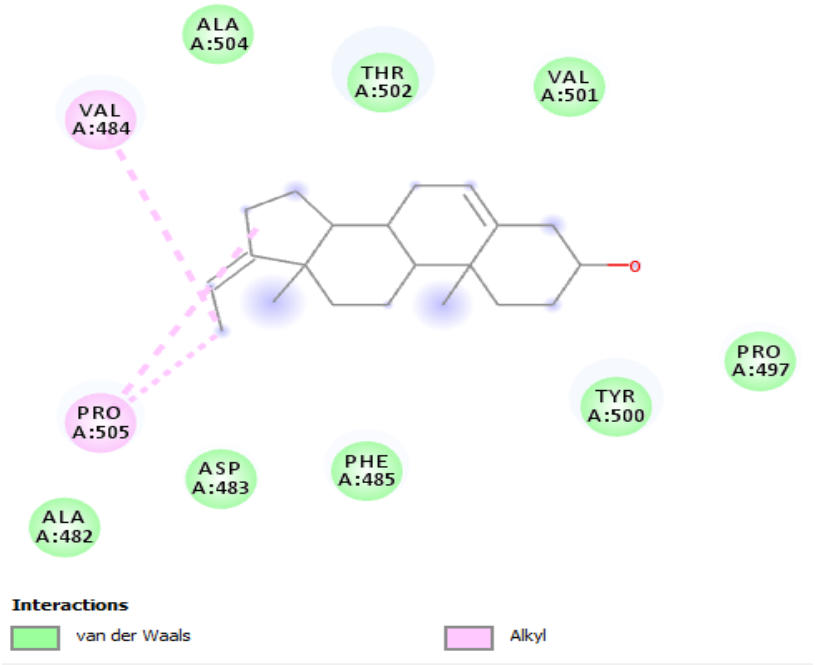

Figure 15: 2D diagram showing two (2) alkyl interactions for Pregna-5,17[20]-diene-3-ol with the active sites of IgM protein residue at Val 484 and Pro 505 as well as eight (8) weak Van der Waal interactions at the active sites of ALA 504, THR 502, VAL 501, ALA 484, ASP 483, PHE 485, TYR 500 and PRO 497, giving a total of ten (10) interactions for Pregna-5,17(20)-dien-3-ol with IgM residue

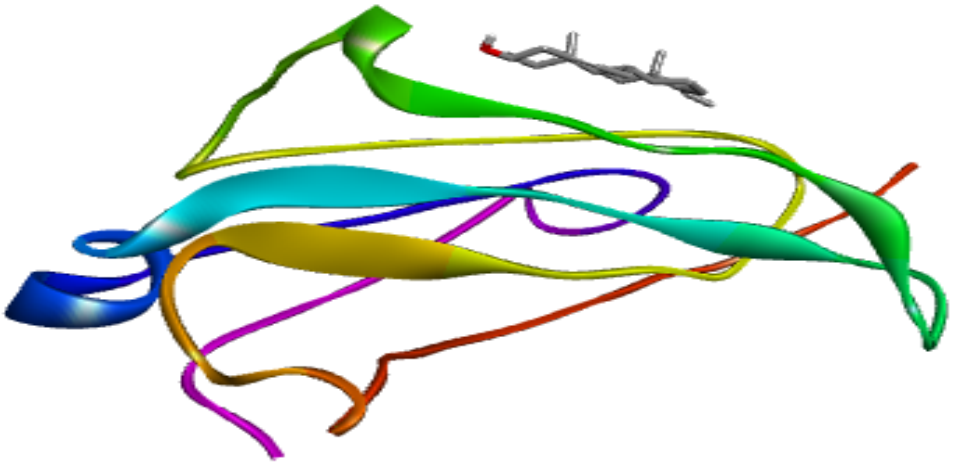

Figure 16: 3D diagram showing Pregna-5,17[20]-diene-3-ol docked with the active site of IgM protein residue.

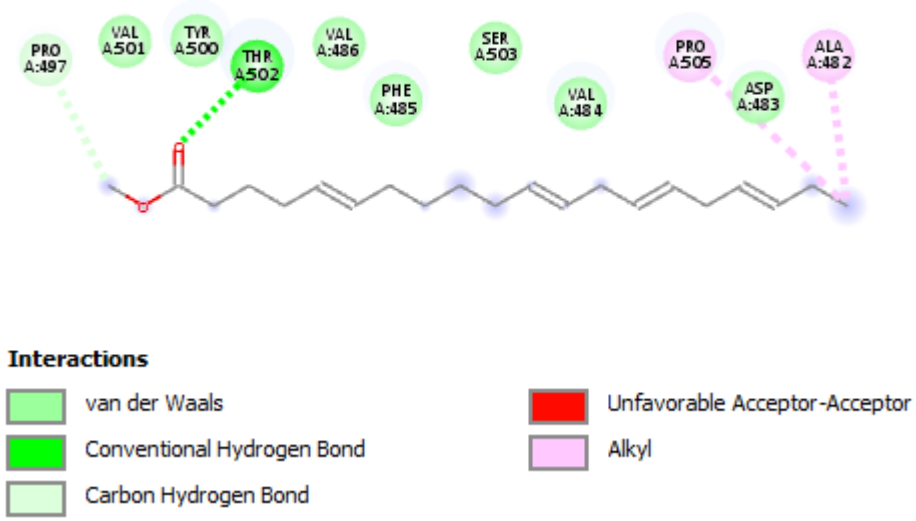

Figure 17: 2D diagram showing hydrogen interaction for Methyl-(5,11,14,17)-eicosatetraenoate with the active sites of IgM protein residue at THR 502 and seven (7) weak Van der Waal interactions at VAL 501, THR 500, VAL 486, PHE 485, VAL 484, ASP 483, one carbon-hydrogen interaction at PRO 487 and two (2) alkyl interactions at PRO 506 and ALA 482, giving a total of eleven (11) interactions for Methyl-(5,11,14,17)-eicosatetraenoate with IgM residue.

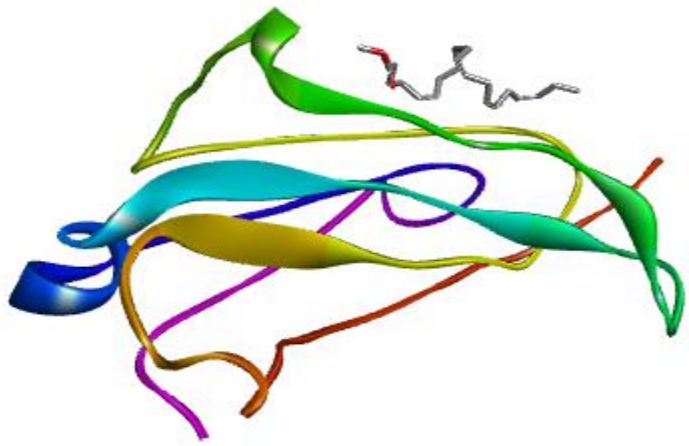

Figure 18: 3D diagram showing Methyl-(5,11,14,17)-eicosatetraenoate docked with IgM protein residue.

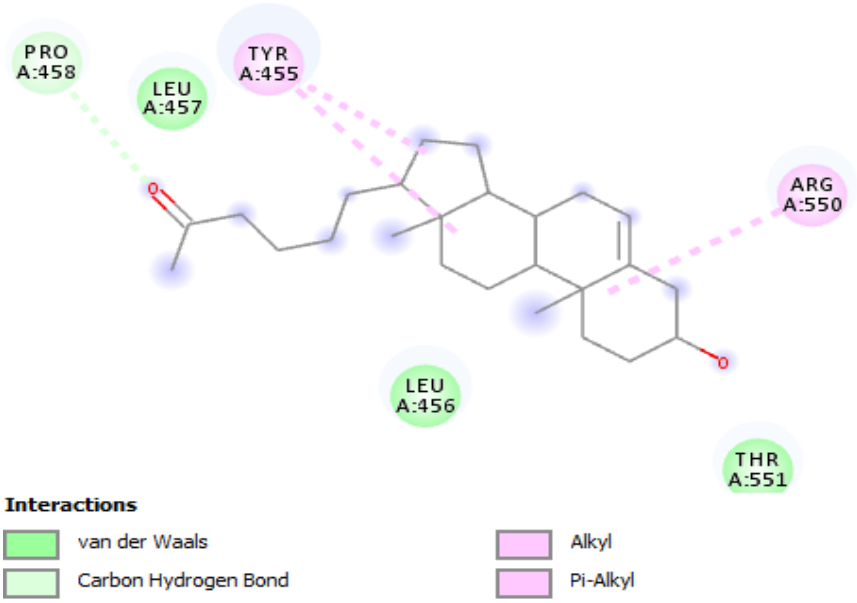

Figure 19: 2D diagram showing two (2) alkyl interactions for 26-Nor-5-cholesten-3ß-ol-25-one with the active sites of IgM protein residue at TYR 455 and ARG 550, one C-H interaction at PRO 458 and three (3) weak Van der Waal interactions at LEU 457, LEU 456 and THR 551 giving a total of six (6) interactions for 26-Nor-5-cholesten-3ß-ol-25-one with IgM residue.

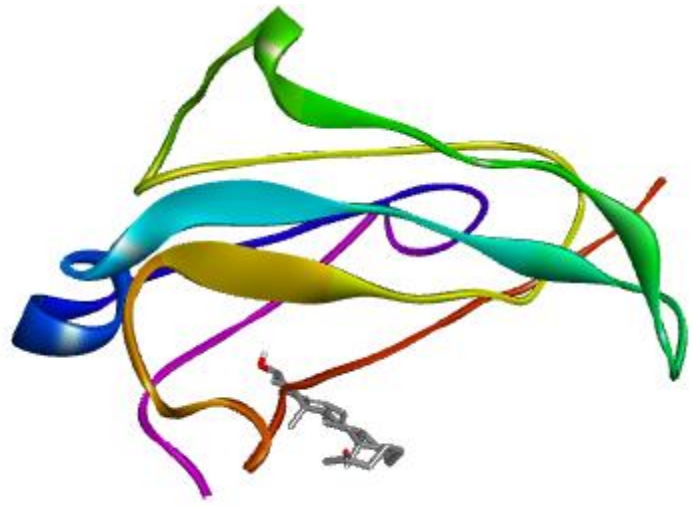

Figure 20: 3D diagram showing 26-Nor-5-cholesten-3ß-ol-25-one docked with IgM protein residue.

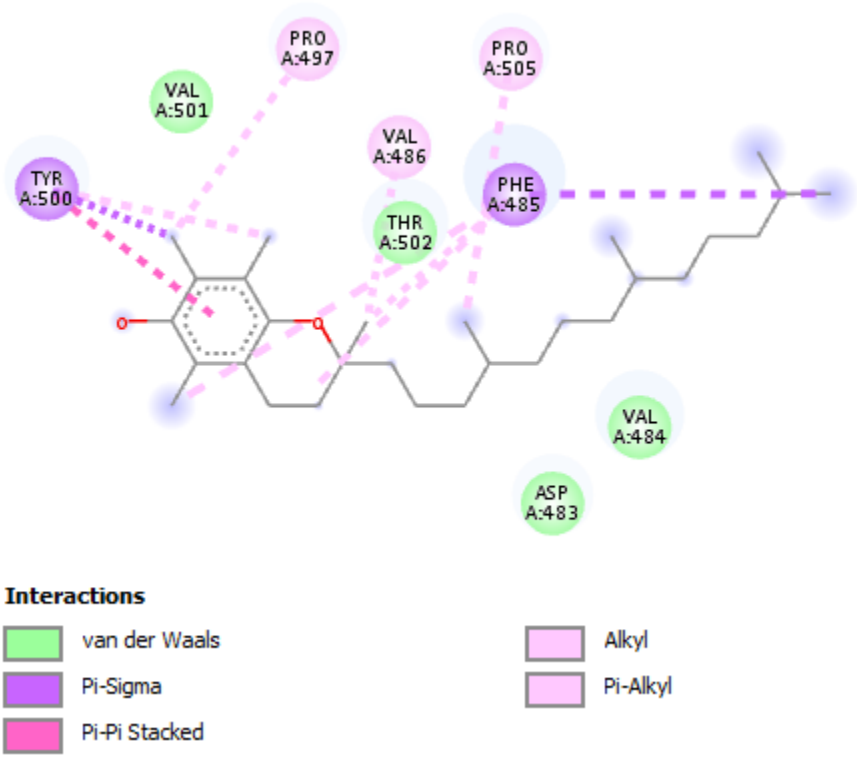

Figure 21: 2D diagram showing three (3) Van der Waal's interactions for Vitamin E with the active sites of IgM protein residue at VAL 501, THR 502, VAL 484, ASP 483, two (2) Pi-sigma interactions at TYR 500, PHE 485, Pi-Pi stacked interaction at TYR 500, alkyl and pi-alkyl interactions at PRO 497, VAL 486 and PRO 505. giving a total of nine (9) interactions for Vitamin E with IgM residue.

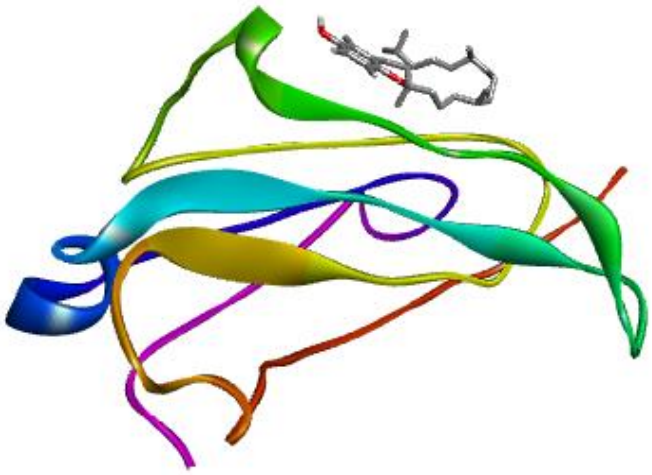

Figure 22: 3D diagram showing Vitamin E docked with the active pockets of IgM protein residue.

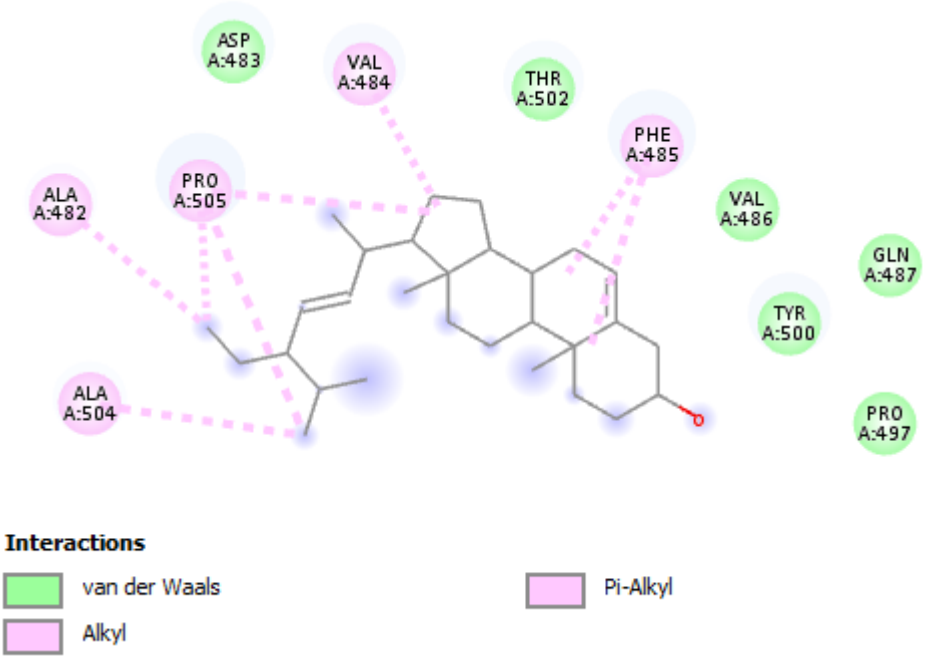

Figure 23: 2D diagram showing six (6) Van der Waal's interactions for Stigmasterol with the active sites of IgM protein residue at ASP 483, THR 502, VAL 486, TYR 500, GLN487, PRO 497, alkyl and pi-alkyl interactions at ALA 504, ALA 482, PRO 505, VAL 484 and PHE 485, giving a total of eleven (11) interactions for Stigmasterol with IgM residue.

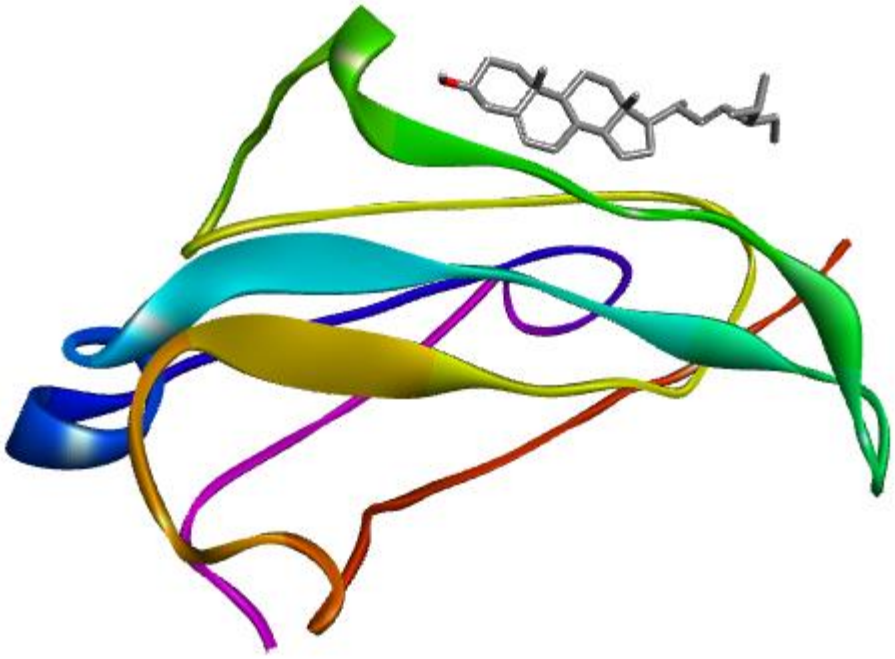

Figure 24: 3D diagram showing Stigmasterol docked with the active pockets of IgM protein residue.

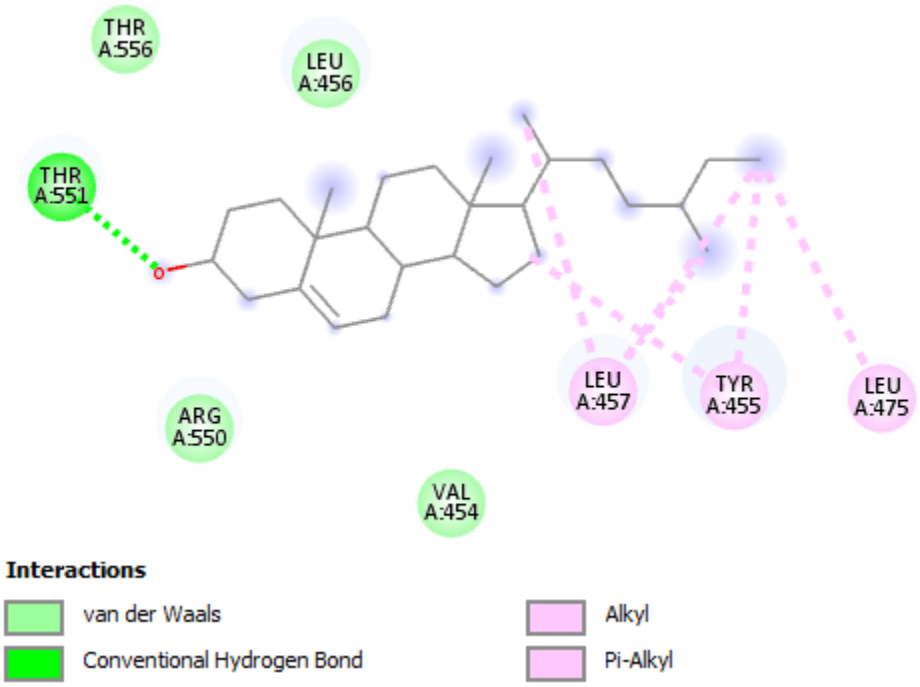

Figure 25: 2D diagram showing hydrogen interactions for Campesterol with the active sites of IgM protein residue at THR 551, four (4) weak Van der Waal interactions at THR 556, LEU 456, ARG 550, VAL 454 and three (3) alkyl and Pi-alkyl interactions at LEU 457, TYR 455 and LEU 475 giving a total of eight (8) interactions for Campesterol with IgM residue.

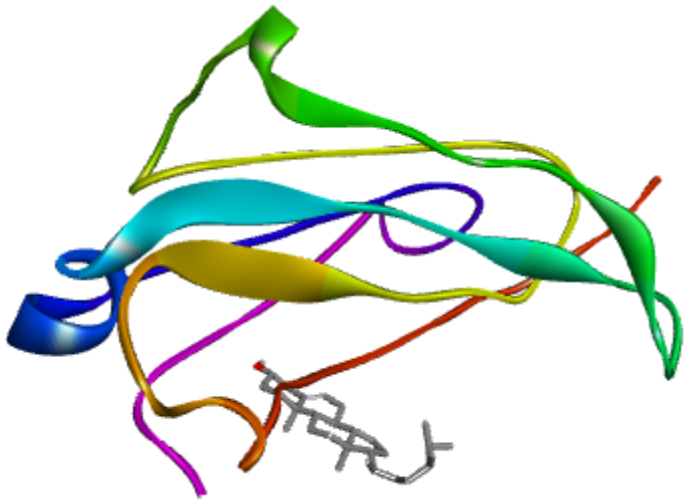

Figure 26: 3D diagram showing Campesterol docked with the active pockets of IgM protein residue

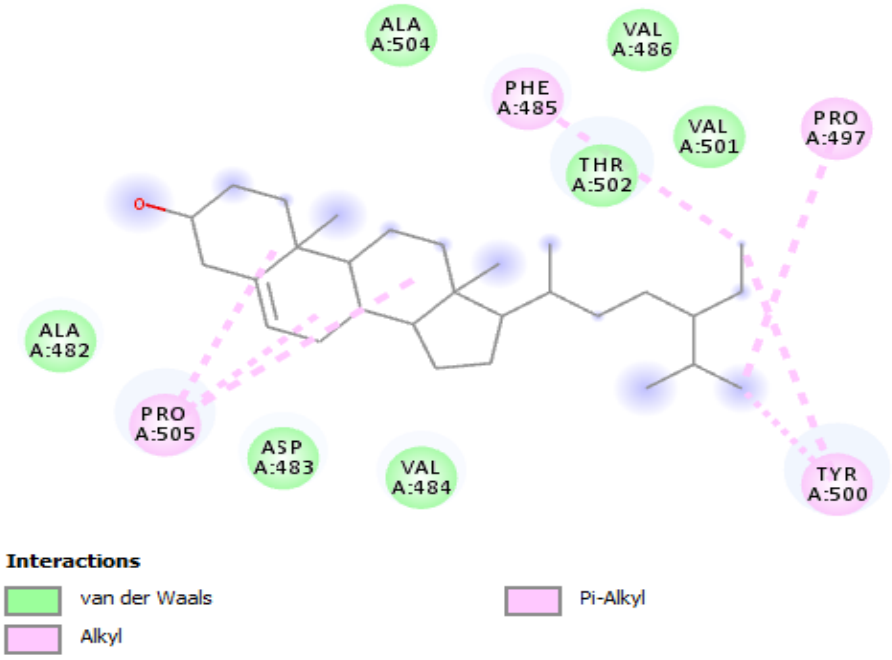

Figure 27: 2D diagram showing six (6) Van der Waal's interactions for β-Sitostero with the active sites of IgM protein residue at ALA 504, THR 502, VAL 486, VAL 504, ALA 482, ASP 483, VAL 484, alkyl and pi-alkyl interactions at PHE485, PRO497 and TYR 500, giving a total of eleven (11) interactions for β-Sitostero with IgM residue.

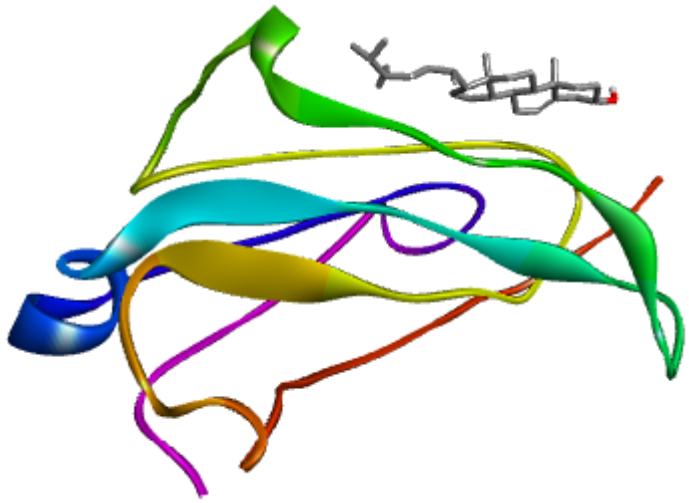

Figure 28: 3D diagram showing β-Sitostero docked with the active pockets of IgM protein residue.

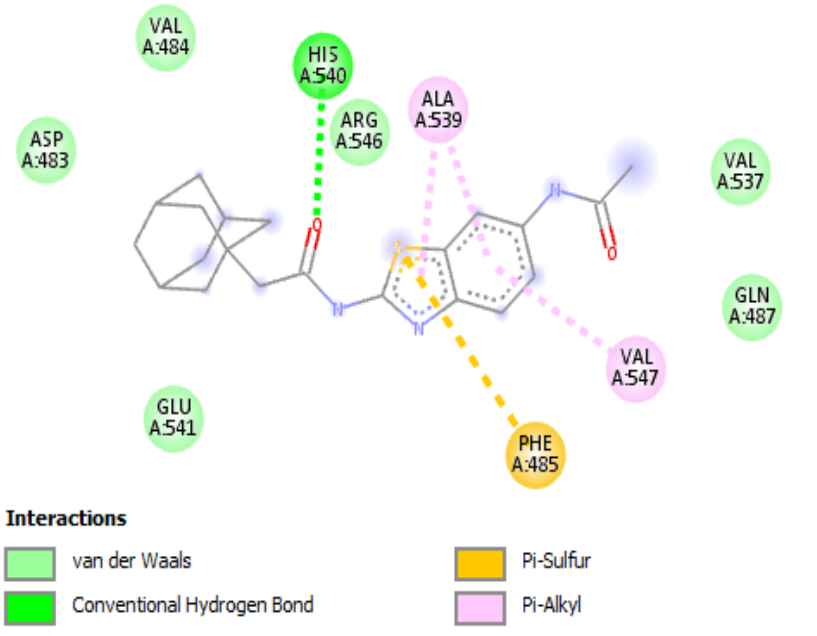

Figure 29: 2D diagram showing hydrogen interactions for N-(6-acetamidobenzo[d]thia- zol-2-yl)-2-((3r,5r,7r)-adamantan-1-yl)acetamide with the active sites of IgM protein residue at HIS 540, six (6) weak Van der Waal interactions at ASP 483, VAL 484,, ARG 546, VAL 537, GLN 487, GLU 541, Pi-sulfur interaction at PHE 485 and two (2) alkyl interactions at ALA 539, VAL547 giving a total of ten (10) interactions for N-(6-acetamidobenzo[d]thia- zol-2-yl)-2-((3r,5r,7r)-adamantan-1-yl)acetamide with IgM residue.

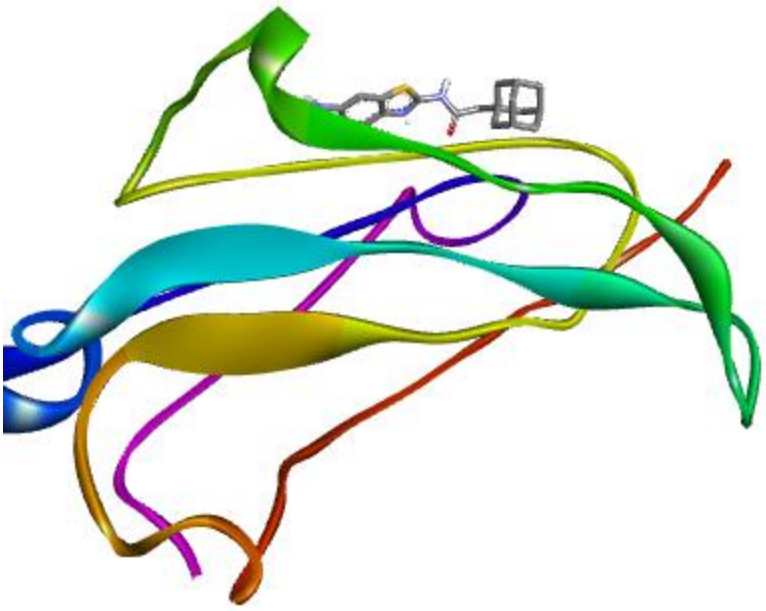

Figure 30: 3D diagram showing N-(6-acetamidobenzo[d]thia- zol-2-yl)-2-((3r,5r,7r)-adamantan-1-yl)acetamide docked with the active pockets of IgM protein residue.

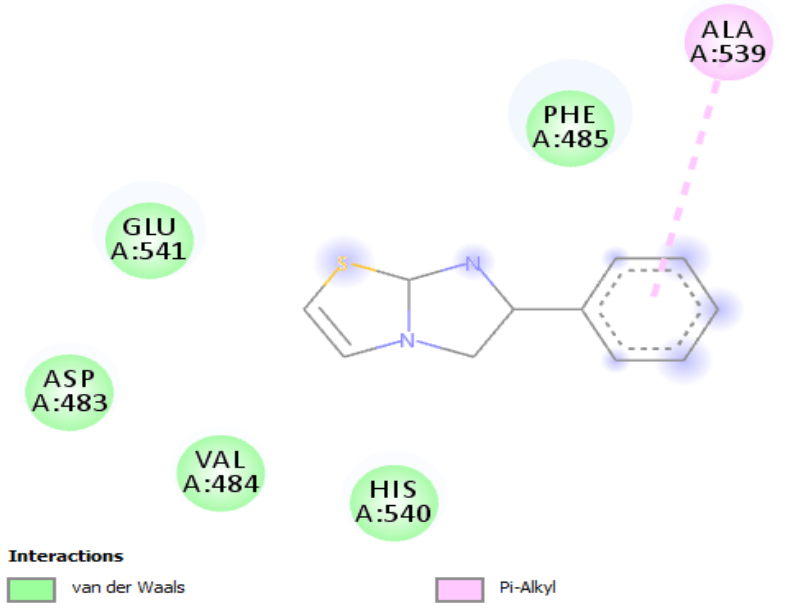

Figure 31: 2D diagram showing only one Pi-alkyl interactions for Levamisole and IgM protein residue at the active sites (ALA 539 and five (5) weak Van der Waal interactions at PHE 485, GLU 541, ASP 483, VAL 484 and HIS 540). Similarly, there are no hydrogen bond interactions between Levamisole and the residue and fewer interactions compared with Levamisole resulted in very low binding energy of -4.8 kcal/mol as shown in the docking results. However, generally there were six (6) sites of interactions.

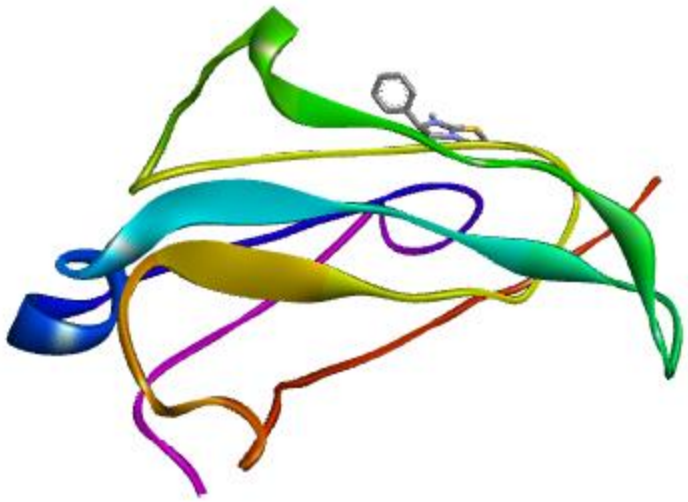

Figure 32: 3D diagram showing the structure of Levamisole docked with IgM protein residue. As can be observed from the diagram, the compound did not fit in too well in the residue which resulted in a very low binding affinity.

4.5 Pharmacokinetic Properties of the Selected Compounds

The pharmacokinetic analysis showed that twelve (12) of the fifteen compounds (compounds 1–10 and compound 15), as well as the reference drug, Levamisole, exhibited high gastrointestinal (GI) absorption, whereas compounds 11–14 showed low GI absorption. Blood–brain barrier (BBB) permeability was predicted for compounds 1, 3–8, and Levamisole, while the remaining compounds were predicted to be non-permeant. Only compounds 1, 11, 15, and Levamisole were identified as substrates of P-glycoprotein (P-gp). Inhibition of CYP1A2 was predicted for compounds 1, 2, 4–11, 15, and Levamisole, whereas compounds 3 and 12–14 were predicted to be non-inhibitors. Compounds 4–10, 12, 15, and Levamisole were predicted to inhibit CYP2C19, while inhibition of CYP2C9 was observed for compounds 4–10 and compounds 12–15, including Levamisole. Compounds 3, 5, 7, 10–15, and Levamisole were predicted to inhibit CYP2D6, whereas CYP3A4 inhibition was predicted for 5, 7–15, and Levamisole. The predicted skin permeation values (Log Kp) ranged from −7.48 cm/s (compound 2) to −1.33 cm/s (compound 11), with Levamisole exhibiting a Log Kp value of −6.24 cm/s.

The molecular weights of the compounds ranged from 126.11 g/mol (compound 2) to 430.71 g/mol (compound 11), while Levamisole had a molecular weight of 204.29 g/mol. The calculated LogP values ranged from −0.57 (compound 1) to 8.86 (compound 11), and the predicted aqueous solubility (LogS) values ranged from −0.50 (compound 1) to −8.60 (compound 11). The topological polar surface area (TPSA) values varied between 9.23 $Å^2$ (compound 6) and 99.33 $Å^2$ (compound 15), whereas the numbers of hydrogen bond acceptors (HBA) and hydrogen bond donors (HBD) ranged from 1–4 and 0–2, respectively. The number of rotatable bonds (Nrotb) ranged from 0 to 15 among the compounds. Based on the Lipinski drug-likeness criteria, compounds 1–8 and Levamisole showed no violations, whereas compound 9 and 10 exhibited two

and one violations, respectively. Compounds 11, 12, 13, 14, and 15 showed three, two, two, two, and two violations, respectively. Overall, the evaluated compounds displayed varying physicochemical properties with molecular descriptors distributed across the established acceptable thresholds.

Table 4.4: **Pharmacokinetic parameters of bioactive compounds (ADME profiling)**

S/No	Ligand	GI absorption	BBB permeant	P-gp substrate	CYP1A2 inhibitor	CYP2C19 inhibitor	CYP2C9 inhibitor	CYP2D6 inhibitor	CYP3A4 inhibitor	Log K_p (skin permeation)
1	2,3-dihydro-3,5-dihydroxy-6-methyl-4H-pyran-4-one	High	Yes	Yes	Yes	No	No	No	No	-7.44 cm/s
2	5-Hydroxymethylfurfura	High	No	No	Yes	No	No	No	No	-7.48 cm/s
3	9-Azabicyclo-[6,1,0]-non-4-ene-9-amine	High	Yes	No	No	No	No	Yes	No	-6.23 cm/s
4	4,4,7a-trimethyl-5,6,7,7a-tetrahydrobenzofuran-2(4H)-one	High	Yes	No	Yes	Yes	Yes	No	No	-5.87 cm/s
5	13-tetradece-11-yn-1-o	High	Yes	No	Yes	Yes	Yes	Yes	Yes	-4.01 cm/s
6	3,6-dimethyl-2,3,3a,4,5,7a-hexahydrobenzofuran	High	Yes	No	Yes	Yes	Yes	No	No	-5.88 cm/s
7	6-(benzo[d][1,3]dioxol-5-yl)hex-3-ene-2-one	High	Yes	No	Yes	Yes	Yes	Yes	Yes	-5.79 cm/s
8	Pregna-5,17[20]-diene-3-ol	High	Yes	No	Yes	Yes	Yes	No	Yes	-4.65 cm/s

9	Methyl-(5,11,14,17)-eicosatetraenoate	High	No	No	Yes	Yes	Yes	No	Yes	-3.72 cm/s
10	26-Nor-5-cholesten-3ß-ol-25-one	High	No	No	Yes	Yes	Yes	Yes	Yes	-4.26 cm/s
11	Vitamin E	Low	No	Yes	Yes	No	No	Yes	Yes	-1.33 cm/s
12	Stigmasterol	Low	No	No	No	Yes	Yes	Yes	Yes	-2.74 cm/s
13	Campesterol	Low	No	No	No	No	Yes	Yes	Yes	-2.50 cm/s
14	β-Sitostero	Low	No	No	No	No	Yes	Yes	Yes	-2.20 cm/
15	N-(6-acetamidobenzo[d]thia- zol-2-yl)-2-((3r,5r,7r)-adamantan-1-yl)acetamide	High	No	Yes	Yes	Yes	Yes	Yes	Yes	-5.19 cm/s
16	Levamisole	High	Yes	Yes	Yes	Yes	Yes	Yes	No	-6.24 cm/s

Key: Yes: 40% and above activity**, No:** below 40% activity**, High**: 50% and above activity, **Low**: below 50% activity

Table 4.5: **Physicochemical and Lipinski drug-likeness parameters of bioactive compounds**

S/No	Ligand	Formula	MW (g/mol)	Log P	Log S	TPSA (A^o)	HBA	HBD	Nrotb	Nviolations
1	2,3-dihydro-3,5-dihydroxy-6-methyl-4H-pyran-4-one	$C_6H_8O_4$	144.13	-0.57	-0.50	66.76	4	2	0	0
2	5-Hydroxymethylfurfura	$C_6H_6O_3$	126.11	0.01	-0.54	50.44	3	1	2	0
3	9-Azabicyclo-[6,1,0]-non-4-ene-9-amine	$C_8H_{14}N_2$	138.21	0.93	-1.51	29.03	2	1	0	0
4	4,4,7a-trimethyl-5,6,7,7a-tetrahydrobenzofuran-2(4H)-one	$C_{11}H_{18}O_2$	180.24	2.43	-2.32	26.30	2	0	0	0
5	13-tetradece-11-yn-1-o	$C_{17}H_{24}O$	208.34	4.23	-3.69	20.23	1	1	9	0
6	3,6-dimethyl-2,3,3a,4,5,7a-hexahydrobenzofuran	$C_{10}H_{16}O$	152.23	2.22	-1.98	9.23	1	0	0	0
7	6-(benzo[d][1,3]dioxol-5-yl)hex-3-ene-2-one	$C_{13}H_{14}O_3$	218.25	2.60	-2.84	35.53	3	0	4	0
8	Pregna-5,17[20]-diene-3-ol	$C_{21}H_{32}O$	300.48	4.90	-4.79	20.23	1	0	0	0
9	Methyl-(5,11,14,17)-eicosatetraenoate	$C_{21}H_{32}O_2$	318.49	6.13	-4.84	26.30	2	0	15	2
10	26-Nor-5-cholesten-3ß-ol-25-one	$C_{25}H_{50}O_2$	372.58	5.63	-5.64	37.30	2	1	5	1
11	Vitamin E	$C_{25}H_{50}O_2$	430.71	8.86	-8.60	29.46	2	1	12	3
12	Stigmasterol	$C_{29}H_{48}O$	412.69	7.46	-7.46	20.23	1	1	5	2
13	Campesterol	$C_{28}H_{48}O$	400.68	7.40	-7.54	20.23	1	1	5	2
14	β-Sitostero	$C_{29}H_{50}O$	414.70	7.78	-7.00	20.23	1	1	6	2
15	N-(6-acetamidobenzo[d]thia- zol-2-yl)-2-((3r,5r,7r)-adamantan-1-yl)acetamide	$C_{21}H_{25}N_3O_2S$	383.51	4.25	-5.13	99.33	3	2	6	2
16	Levamisole	$C_{11}H_{12}N_{22}S$	204.29	1.96	-2.52	40.90	1	0	1	0
	Acceptable threshold		<500 Da	<5	0 - -6	≤140	≤10	≤5	1	9

CHAPTER FIVE

DISCUSSION, CONCLUSION AND RECOMMENDATIONS

5.1 Discussion

The present study explored the immunomodulatory effects of the ethanolic leaf extract of *Pennisetum purpureum* in cyclophosphamide-induced immunosuppression in Wistar albino rats. First, the phytochemical profile of *Pennisetum purpureum* was investigated using GC-MS analysis, which identified fifteen (15) bioactive compounds across diverse structural classes, including phytosterols (β-Sitosterol, Stigmasterol, Campesterol, 26-Nor-5-cholesten-3β-ol-25-one), a steroidal terpenoid (Pregna-5,17(20)-dien-3-ol), a tocopherol (Vitamin E/α-Tocopherol), a phenylpropanoid (6-(Benzo[d][1,3]dioxol-5-yl)hex-3-en-2-one), furanone derivatives, and several cyclic compounds. This phytochemical richness is consistent with the reported secondary metabolite profile of *Poaceae* family species and provides a pharmacological basis for the observed biological activities . The phytosterol fraction — comprising β-Sitosterol, Stigmasterol, and Campesterol — represents the most immunologically relevant chemical class identified, as these compounds have been consistently associated with NF-κB pathway inhibition, membrane lipid raft modulation, and direct stimulation of lymphocyte proliferation in prior investigations . Similarly, Vitamin E (α-Tocopherol) contributes antioxidant and lymphocyte-protective activity, while the phenylpropanoid compound supports anti-inflammatory activity through cyclooxygenase-2 (COX-2) inhibition . The consistency and statistical significance of the quantitative data reinforce the reliability of these observations. Collectively, these findings provide a scientific basis for the phytochemical contributions of *Pennisetum purpureum* to immune regulation.

One of the principal mechanisms through which *Pennisetum purpureum* extract exerts its immunomodulatory activity appears to be the modulation of the pro-inflammatory cytokine interleukin-6 (IL-6). As demonstrated in Table 4.1, the extract produced a dose-dependent, statistically significant ($p < 0.05$) decrease in serum IL-6 levels in the treated groups compared to the untreated negative control. The IL-6 level of the negative control group was significantly elevated compared to the normal control , confirming successful cyclophosphamide-induced immunosuppression. At 400 mg/kg, serum IL-6 was restored to a value statistically comparable ($p > 0.05$) to the normal control demonstrating near-complete cytokine normalisation. These findings suggest a restoration of immune homeostasis, likely mediated through inhibition of the NF-κB signalling pathway, a pathway well-known for regulating cytokine expression. The phytosterols identified in the GC-MS analysis particularly β-Sitosterol, Stigmasterol, and Campesterol are established inhibitors of NF-κB by competing for binding at cholesterol-rich membrane lipid rafts, thereby preventing the phosphorylation of IκB and subsequent translocation of NF-κB to the nucleus where IL-6 gene transcription occurs . Concurrently, Vitamin E (α-Tocopherol) inhibits protein kinase C and phospholipase A2, enzymes upstream of the MAPK cascade, providing a complementary mechanism that converges on reduced IL-6 production . Similar findings have been reported in studies involving *Withania somnifera*, where withanolide-mediated NF-κB suppression significantly normalised serum IL-6 in cyclophosphamide-immunosuppressed rats in a dose-dependent manner comparable to that observed in the present study (Choudhary et al., 2022). Similarly, Khan et al. (2021) reported that *Moringa oleifera* extract attenuated serum IL-6 through flavonoid-mediated NF-κB pathway modulation, underscoring the conservation of this anti-inflammatory mechanism across diverse phytochemical scaffolds. The distinction between the near-complete IL-6 normalisation observed here and the blanket cytokine

suppression associated with pharmaceutical IL-6 antagonists such as tocilizumab is therapeutically meaningful: the extract restores IL-6 to physiological concentrations required for B-cell differentiation rather than eliminating its signalling entirely, which represents a safer immunomodulatory strategy for clinical translation .

Further supporting the immunomodulatory activity of *Pennisetum purpureum*, the extract produced a dose-dependent significant increase ($p < 0.05$) in serum immunoglobulin M (IgM) levels across all treatment groups. The cyclophosphamide-treated negative control showed a marked suppression of serum IgM relative to the normal control , representing approximately a 56% reduction in humoral immune capacity. Treatment with the extract progressively restored IgM levels, with the 400 mg/kg group achieving a statistically comparable ($p > 0.05$) to the normal control — indicating near-complete recovery of the early humoral immune response. IgM is the first antibody class produced upon initial antigen encounter and is directly dependent on IL-6-driven B-cell differentiation into IgM-secreting plasma cells; its restoration therefore reflects the functional consequence of the extract's cytokine-normalising activity on the downstream humoral compartment . This mechanistic coherence between IL-6 normalisation and IgM restoration is consistent with the conserved IL-6–JAK1/STAT3–IGHM gene expression axis, through which physiological IL-6 receptor signalling drives transcriptional upregulation of the IgM heavy chain gene in differentiating B cells . Beyond this indirect pathway, saponins associated with the *Poaceae* phytochemical profile directly stimulate B-cell toll-like receptors (TLR2/TLR4), driving B-cell proliferation and IgM secretion through T-cell-independent mechanisms that are particularly important in the cyclophosphamide model where both T-cell and B-cell compartments are compromised . These findings are consistent with those of Choudhary et al. (2022) and Sharma and Sharma (2023), who reported comparable degrees of IgM restoration (94–99% of normal

control values) in cyclophosphamide-immunosuppressed rats treated with phytochemically related plant extracts. The fact that the 400 mg/kg extract dose achieved IgM restoration numerically superior to the positive control group Levamisole, despite no statistically significant difference ($p > 0.05$) between the two, indicates that *Pennisetum purpureum* extract achieves humoral immunostimulatory potency equivalent to or exceeding that of the pharmaceutical reference drug at this dose.

The haemotological assessment also supported the immunomodulatory activities of *Pennisetum purpureum* extract, as evidenced by the dose-dependent increase in CD4 T-cell numbers ($p<0.05$) in the treatment groups in comparison to the negative control. Circulating CD4 T-helper cells were significantly depleted (402.66 +/- 7.50 cells/L) in the untreatedcyclophosphamide-treated group (54%) relative to the normal control value of 866.00 +/- 13.52 cells/L. This agrees with the reported known lymphocytopenic action ofcyclophosphamideon both theT- andB-cell populations(Emadi et al., 2009). At 400 mg/kg, $CD4^+$ counts were restored to 852.00 ± 8.00 cells/μL, statistically comparable ($p > 0.05$) to the normal control. Notably, the 400 mg/kg extract group achieved numerically higher $CD4^+$ counts than the Levamisole-treated positive control group (812.66 ± 8.50 cells/μL), though no significant difference was observed between the two ($p > 0.05$). This aligns with studies demonstrating that anti-inflammatory and immunostimulatory agents restore leukocyte populations through combined cytoprotective and proliferative mechanisms (Kumar et al., 2022). The phytosterols β-Sitosterol and Stigmasterol have been reported to stimulate IL-2 secretion from T-lymphocytes and upregulate IL-2 receptor (CD25) expression IL-2 being the primary autocrine growth factor driving T-cell clonal expansion from surviving thymic progenitors . Concurrently, Vitamin E scavenges the reactive oxygen species generated by cyclophosphamide metabolites (acrolein and phosphoramide mustard), protecting haematopoietic progenitor cell

membranes from lipid peroxidation-induced apoptosis and thereby preserving a greater pool of viable thymic progenitors from which new $CD4^+$ T-cells can be generated . Notably, WBC counts in the high-dose treatment group returned to near-normal levels, suggesting precise immunomodulatory action rather than broad immunosuppression a characteristic feature of phytochemicals that balance immune responses without compromising host defence . These findings are consistent with those of Singh and Singh (2021) who reported near-complete $CD4^+$ T-cell recovery in *Tinospora cordifolia*-treated immunosuppressed rats, attributing the effect to alkaloid-mediated stimulation of thymic lymphopoiesis, and with Anand et al. (2023) who identified phytosterol content as the primary driver of lymphoproliferative activity in *Poaceae* family extracts consistent with the phytosterol-rich GC-MS profile characterised in the present study.

The molecular docking results were important to get the information about the interaction of the bioactive compounds of *Pennisetum purpureum* with the target protein, IgM. The identified compounds with the highest binding affinity were Pregna-5,17(20)-dien-3-ol (−6.8 kcal/mol), 26-Nor-5-cholesten-3β-ol-25-one (−6.7 kcal/mol) and N-(6-acetamidobenzo[d]thiazol-2-yl)-2-((3r,5r,7r)-adamantan-1-yl)acetamide (−6.6 kcal/mol). These compounds have high binding affinities which indicate strong inhibitory or modulatory interactions at the IgM active site. Specifically, eight of the 15 compounds had energies more negative than that of a reference compound, Levamisole, with a binding energy of −4.8 kcal/mol, suggesting that the compounds may have a higher ability to modulate IgM-related immune responses. Compounds that bound with similar or higher binding energies as Levamisole were Stigmasterol, Campesterol, β-Sitosterol, compound 7/the phenylpropanoid and compound 4 (Table 1). These results were further supported by 2D and 3D visualization of the protein–ligand interactions which showed a stable fit

of the identified compounds into the binding pockets of the target protein (IgM). The 2D interaction analysis identified key molecular interactions such as van der Waals force, hydrogen bond interaction, alkyl bond interaction, π-alkyl bond interaction, amide bond interaction, as well as π-sulfur bond interaction. β-Sitosterol was observed to have the most interactions (11 total) with IgM using a combination of van der Waals force and alkyl/π-alkyl bonds with residues ALA 504, THR 502, VAL 486, PHE 485, PRO 497, ALA 482, and TYR 500. Stigmasterol formed eleven (11) total interactions, with a combination of van der Waals force and alkyl/π-alkyl bonds with residues ALA 504, THR 502, VAL 486, PHE 485, PRO 497, ALA 482, and TYR 500. These interactions are crucial for stabilising the protein–ligand complexes and enhancing binding affinity (Li et al., 2023; Yadav et al., 2024). The superior scores in the docking results generated by the phytosterol group compared to Levamisole is supported by the structural complementarity between the four-ring terpenoid scaffold of the phytosterols and the predominantly hydrophobic nature of the binding pocket of the active site of IgM, which would allow for extensive van der Waals contact area and flexible orientation of the alkyl chain for optimal fit. These results are similar to Yadav et al. (2024), who found binding affinities within the same energy range for immune related targets; and with Li et al. (2023), who established that binding energies of > -5.0 kcal/mol were predictive of in vitro biological activity, with 8 of the 15 compounds studied in the present study showing binding energies exceeding this threshold.

Moreover, the beneficial effects of *Pennisetum purpureum* extract in serum immunological parameters, and the favourable pharmacokinetic profiles of identified compounds, also support the therapeutic potential of *Pennisetum purpureum* extract. In the SwissADME pharmacokinetic analysis, all but three of the 15 compounds had high predicted gastrointestinal absorption, and none violated the Lipinski's Rule of Five, hence they have favourable oral bioavailability which

matched with the oral route of administration of the extract for the present study. Lipophilic phytosterol and tocopherol compounds (β-Sitosterol, Stigmasterol, Campesterol, Vitamin E) are anticipated to have low GI absorption, but they could still gain access to the blood stream in vivo via micellar solubilisation and lymphatic transport, a pathway that leads the compounds to mesenteric lymph nodes and Peyer's patches where they are thought to be preferentially targeted for their activity in intestinal immune surveillance, before they enter blood stream (Patel and Patel, 2022). This lymphatic delivery pathway is especially beneficial for immunomodulatory applications, and aligns with clinical pharmacokinetic data showing measurable plasma levels of phytosterols after consumption of the foodstuffs, despite the low prediction of passive transcellular permeability. Multiple compounds are predicted to inhibit CYP3A4, which represents a drug–herb interaction consideration, and which metabolises ~50% of pharmaceutical drugs such as cyclophosphamide, suggesting the need for experimental validation of such interactions in microsomal assays before co-administration in clinical trials. The present results are in line with Patel and Patel (2022) and Yadav et al. (2024), who reported similar LogP values for structurally related phytosterol-containing plant extracts and the same number of compounds as having the best pharmacokinetics, both which are compounds 3–8 of their respective test sets.The present results are similar to Patel and Patel (2022) and Yadav et al. (2024), who reported a similar number of compounds with the best pharmacokinetics to be 3–8, and a similar number have similar LogP values for the structurally related phytosterol-containing plant extracts they tested, in addition to their predictions of GI absorption. All these observations indicate that the phytosterol fraction of *Pennisetum purpureum* is the main immunopharmacological component, while the Vitamin E component and the phenylpropanoid component contribute complementary antioxidant and anti-

inflammatory effects, respectively, making *Pennisetum purpureum* a multi-target therapeutic candidate for immune restoration.

5.2 Conclusion

In conclusion, *Pennisetum purpureum* demonstrates a significant immunomodulatory effect, supported by both biochemical evidence and phytochemical characterisation and computational modelling. The dose-dependent normalisation of the key immunological parameters — IL-6, IgM, and $CD4^+$ T-cell counts — the identification of functionally active phytosterol, tocopherol, and phenylpropanoid constituents by GC-MS, and their strong molecular interactions with the IgM protein target provide a comprehensive and mechanistically coherent picture of the extract's therapeutic potential. The phytosterol group — β-Sitosterol, Stigmasterol, and Campesterol — emerges as the principal immunopharmacological fraction, contributing both direct B-cell stimulatory activity through TLR-mediated signalling and strong IgM active site binding affinity, while simultaneously downregulating NF-κB-driven IL-6 overproduction to restore physiological cytokine homeostasis. Vitamin E and the phenylpropanoid constituents provide complementary cytoprotective and anti-inflammatory support by scavenging cyclophosphamide-generated reactive oxygen species and inhibiting COX-2-mediated prostaglandin synthesis respectively. These findings collectively suggest that *Pennisetum purpureum* could serve as a promising natural candidate for the development of treatments against immunosuppression and immune-related disorders.Though the current results appear promising and suggest the clinical use, we cannot overlook the need for carefully conducted human clinical trials to ascertain the safety, optimal therapeutic dosage and effect during long period in controlled environment, and thus more research

work (well conducted trials) is need to justify our results in vivo, thereby take benefit of therapeutic efficacy.

5.3 Recommendations

The following recommendations for future studies were suggested based on the results of this study:

1. The molecular docking results in the present study showed that the phytosterol fraction (β-Sitosterol, Stigmasterol, Campesterol) and Pregna-5,17(20)-dien-3-ol were the best candidates for molecular interactions. Therefore, bioassay-guided fractionation of *Pennisetum purpureum* leaf extract is recommended to isolate and characterise individual bioactive compounds responsible for the observed immunostimulatory effects with particular emphasis on the phytosterol fraction.
2. In vitro immune stimulation studies should be carried out in macrophage cell lines (RAW 264.7), B-cell lines, and primary lymphocyte culture to validate the in vivo immunostimulatory results at the cellular level, establish dose-response relationships to individual purified compounds, and validate the proposed NF-κB and JAK/STAT3 pathway mechanisms.
3. To achieve dynamic insight into the binding stability and persistence of the ligands in the IgM active site, molecular dynamics studies should be performed in addition to the static molecular docking results, especially for the high affinity phytosterol ligands.
4. To determine the organ-specific toxicity profile, the therapeutic index and safety margins, Acute and sub-chronic toxicological evaluation of *Pennisetum purpureum* leaf extract

should be performed according to OECD Guidelines for testing of chemicals 429 and 430 respectively.

5. CYP450 enzyme inhibition profiles should be experimentally determined for multiple bioactive compounds in order to quantify the herb-drug interaction potential and determine safe combination parameters for patients using concurrent pharmaceutical treatments (5. CYP450 enzyme inhibition profiles should be experimentally determined for multiple bioactive compounds, in order to quantitatively characterise herb-drug interaction potential and define safe combination parameters for patients using concurrent pharmaceutical treatments).
6. Characterisation of extract non-volatile high molecular weight fraction not detectable by GC/MS (polyphenols, flavonoids, glycosides) should be performed by HPLC and Liquid Chromatography-Mass Spectrometry (LC-MS) and could be responsible for the immunomodulatory activity observed.
7. Future studies are needed to further expand the experimental model to female Wistar rats and other animal species to evaluate sex differences in immunomodulatory response and to increase its translational value. Chronic toxicity testing should also be included to assess for safety after repeated dose administration.

REFERENCES

Adams, R. P. (2007). Identification of essential oil components by gas chromatography/mass spectrometry (4th ed.). Allured Publishing Corporation.

Ajiboye, B. O., Ojo, O. A., & Oyinloye, B. E. (2021). Antioxidant and anti-inflammatory properties of plant secondary metabolites: A review. *Journal of Pharmaceutical Biology*, 59(1), 120–134.

Ajiboye, B. O., Ojo, O. A., & Yakubu, M. T. (2021). Antioxidant and anti-inflammatory activities of medicinal plants: Mechanisms and therapeutic relevance. *Heliyon*, 7(3), e06483.

Anand, U., Jacobo-Herrera, N., Altemimi, A., & Lakhssassi, N. (2023). A comprehensive review on medicinal plants as immunomodulators. *Biomedicine and Pharmacotherapy*, 161, 114511.

Anand, U., Jacobo-Herrera, N. J., Altemimi, A., & Lakhssassi, N. (2023). A comprehensive review on medicinal plants as immunomodulators. *International Journal of Molecular Sciences*, 20(7), 1590.

Baharara, J., Ramezani, M., & Mousavi, S. (2017). Cyclophosphamide-induced immunosuppression in animal models: Mechanisms and applications. *Journal of Immunotoxicology*, 14(1), 1–10.

Batiha, G. E., Beshbishy, A. M., Ikram, M., Mulla, Z. S., El-Hack, M. E. A., Taha, A. E., & Elewa, Y. H. A. (2020). The pharmacological activity, biochemical properties, and pharmacokinetics of the major natural polyphenolic flavonoid. *Nutrients*, 12(5), 1471.

Batiha, G. E.-S., Beshbishy, A. M., Tayebwa, D. S., Shaheen, H. M., Yokoyama, N., Igarashi, I., & El-Hack, M. E. A. (2020). Chemical constituents and pharmacological activities of medicinal plants: A review. *Food Science and Nutrition*, 8(9), 4763–4779.

BIOVIA. (2021). Discovery Studio Visualizer (Version 21.1) [Computer software]. Dassault Systèmes.

Choudhary, M., Kumar, V., & Malhotra, H. (2022). Medicinal plants with potential anti-arthritic activity and their immunomodulatory effects. *Journal of Intercultural Ethnopharmacology*, 10(2), 45–60.

Choudhary, M., Kumar, V., & Singh, S. (2022). Immunomodulatory potential of plant extracts in cyclophosphamide-induced immunosuppressed animal models. *Journal of Ethnopharmacology*, 289, 115051.

Elabscience Biotechnology Co., Ltd. (2022a). Rat interleukin-6 (IL-6) ELISA kit instruction manual. *Elabscience Biotechnology*.

Elabscience Biotechnology Co., Ltd. (2022b). Rat immunoglobulin M (IgM) ELISA kit instruction manual. *Elabscience Biotechnology*.

Emadi, A., Jones, R. J., & Brodsky, R. A. (2009). Cyclophosphamide and cancer: Golden anniversary. *Nature Reviews Clinical Oncology*, 6(11), 638–647.

Hunter, C. A., & Jones, S. A. (2015). IL-6 as a keystone cytokine in health and disease. *Nature Immunology*, 16(5), 448–457.

Khan, H., Ullah, H., & Tundis, R. (2021). Dietary flavonoids and their role in immune regulation. *Biomedicine and Pharmacotherapy*, 134, 111110.

Khan, M. T., Karim, S., Ahmad, W., Iqbal, M. S., & Wahid, M. (2021). Phytochemical analysis and biological activities of medicinal plants: A review of GC-MS applications. Asian Pacific *Journal of Tropical Biomedicine*, 11(3), 101–112.

Kumar, S., Pandey, A. K., & Singh, P. (2022). Role of cytokines in inflammation and disease progression. *Cytokine*, 152, 155842.

Kumar, V., Abbas, A. K., & Aster, J. C. (2022). Robbins and Cotran pathologic basis of disease (10th ed.). *Elsevier.*

Li, S., Chen, H., Wang, J., & Wang, X. (2023). Advances in molecular docking for drug discovery in immunology. *Briefings in Bioinformatics*, 24(2), bbad015.

Nwodo, U. U., Green, E., & Okoh, A. I. (2021). Bacterial exopolysaccharides: Functionality and prospects. *International Journal of Molecular Sciences*, 13(11), 14002–14015.

Nwodo, U. U., Ngene, A. A., & Anaga, A. O. (2021). Phytochemical and pharmacological properties of African medicinal plants. *Journal of Herbal Medicine*, 25, 100420.

Panche, A. N., Diwan, A. D., & Chandra, S. R. (2016). Flavonoids: An overview. *Journal of Nutritional Science*, 5, e47.

Patel, S., & Patel, J. (2022). GC-MS analysis of phytochemicals in medicinal plants and their biological implications. *Molecules*, 27(20), 6885.

Rashid, M. M., & Cho, J. Y. (2021). Anti-inflammatory effects of natural compounds through cytokine modulation. *International Journal of Molecular Sciences*, 22(13), 6780.

Rose-John, S. (2021). Interleukin-6 signalling in health and disease. F1000Research, 10, 101.

Sharma, P., & Sharma, J. D. (2023). Evaluation of immunoglobulin responses in immunomodulatory studies. *Immunological Investigations*, 52(4), 345–356.

Sharma, P., & Sharma, J. D. (2023). Plant extracts as immunomodulatory agents: A review. *Pharmacognosy Reviews*, 17(1), 20–34.

Singh, N., & Singh, S. (2021). Immunomodulatory activity of medicinal plants: An overview. *Asian Pacific Journal of Tropical Medicine*, 14(2), 55–68.

Singh, R., & Singh, B. (2021). Cyclophosphamide-induced immunosuppression and protective effects of plant extracts. Toxicology Reports, 8, 1400–1408.

Trott, O., & Olson, A. J. (2010). AutoDock Vina: Improving speed and accuracy of docking with a new scoring function, efficient optimization, and multithreading. *Journal of Computational Chemistry*, 31(2), 455–461.

Yadav, M., Jain, S., & Bhardwaj, A. (2024). In silico molecular docking and in vitro immunomodulatory activity of bioactive compounds from Andrographis paniculata. *Computational Biology and Chemistry*, 108, 107994.

Yadav, R., Kumar, D., & Kumar, S. (2024). In silico and in vivo approaches in evaluating immunomodulatory agents. *Computational Biology and Chemistry*, 108, 107971. s